nature portfolio

Peer Review File

Glypican-3-targeted macrophages delivering drug-loaded exosomes offer efficient cytotherapy in mouse models of solid tumours

REVIEWER COMMENTS

Reviewer #1 (Remarks to the Author):

Comment to Editor

The manuscript entitled as “On-demand editing macrophages enable specific phagocytosis and drug exosome generation for solid tumour cytotherapy” is a very original and well-conceived study. However, this study fails to prove an important point. Organization within a single figure (especially Fig. 2) makes it difficult to understand the content. In addition, the paper is riddled with inappropriate abbreviations (G12, DG12, RILO-M1-G, and RILO-M1-G (RAW264.7) ext.), and then that makes it difficult to understand. Authors would do well to organize the arrangement of the results.

Major
1. Authors have not been able to prove that each compound (R848 or INCB) is contained in RILO. On Supplementary Table 1, it was measured the concentration of vesicles and compounds dissolving in the liquid. Authors shown the stability of vesicles in Supplementary Fig. 2, but how much of the compound remains in the vesicle?
2. The various names for macrophages in this paper are not very good. For example, M1-macrophage (RAW264.7), TAM, M2 macrophages, M1 in HCM etc.
The results of RAW264.7 and bone marrow-derived macrophages should be organized.
3. The use of figure legend abbreviations should be reviewed.

Minor
1. Could TEM results be different from vesicles? For example, Fig. 2e and Fig. 3

Reviewer #2 (Remarks to the Author):

This work with extensive experimental results has merit, and the following are recommended to be addressed in order to maximize its impact:
1. The whole text needs to be carefully reviewed for incomplete sentences, several of which were spotted across the manuscript.
2. All the figure captions should be carefully reviewed to make sure that every panel has a caption and that the caption text
and letter align with their panel.
3. It is unclear why the number of biological replicates for the in vivo experiments were varied (some n=3, others n=5 or n=6). Was there a statistical analysis done to determine how many replicates were needed for significance?
4. It is unclear why statistical significance was processed using one-way ANOVA with Bonferroni correction -- this needs to be better justified, as the validity of the results hinges on this analysis being done properly.
5. It is a bit unclear how the results with this one particular cancer (HCC) and the proposed particular macrophage manipulation would translate into a broader application. The Conclusion states that the components of RILOs and DG12 could "easily be incubated with isolated and purified autologous or allogeneic macrophages in vitro before patient use." Yet this methodology was not tested in this study with the mice.

Reviewer #3 (Remarks to the Author):

In this manuscript, Liu et al. developed innovative on-demand editing macrophages by incorporating surface glypican-3 (GPC3) peptide anchoring and inner lipid particle packing to effectively combat solid tumors. The ingenious modification of cells achieved effective phagocytosis

and reversal of the tumor microenvironment, demonstrating both scientific significance and practical value. Particularly noteworthy was the discovery that the membrane-modified targeting ligand on the surface of living macrophages could be transferred to extracellular vesicles, enabling tumor-targeted uptake and suggesting a novel mechanism for drug release from living cells. This study serves as an inspiration for the development of a new generation of macrophage-based cytotherapy. However, some issues needed to be addressed to further improve the manuscript before publication:

1.The GPC3 peptide G12 is the key ligand for the targeting action of macrophages in the manuscript. The authors suggested that GPC3 peptide G12 has superior specific targeting ability for H22 cells in the preliminary work. Please provide detailed discussion of the preliminary work and key results related to the GPC3 peptide G12 in the "Introduction" or "Conclusions" section. Meanwhile, the application scope of G12 peptide needs to be introduced.

2.Outer membrane vesicles (OMVs) from Escherichia coli were used for improving the drug loading of macrophage-based formulations. Please address safety concerns regarding the use of OMVs considering their bacterial origin.

3.In Fig. 2b and Supplementary Fig. 1, the TAM polarization effect was excellent when the mass ratio of R848 to INCB024360 was between 6:5 and 6:6. Please confirm whether the ratio of R848 to INCB024360 remained between 6:5 and 6:6 upon release.

4.In this manuscript, the authors made efforts to improve the treatment of hepatocellular carcinoma. However, the results in Fig. 4h showed that the accumulation of drugs in the liver was reduced compared with other groups. Please clarify the reason.

5.As shown in the part of "3", it was mentioned that "compared with C6-LO and C6 released from LO-M1 groups, the fluorescence intensity of C6 released from LO-M1-G group showed no significant difference (Fig. 4c,d), which suggested that C6 released from LO-M1-G could be ingested by TAM as expected". Please explain the rationale for selecting the C6-LO group as the control for the LO-M1-G group.

6.Please provide insights into the source of macrophages when applying this strategy to human subjects.

7.Please provide detailed methods for the screening process about the optimal concentration of C16-ceramide in Fig. 1c.

8.As shown in the part of "3", the description of "we found that the RI-exosomes accumulated at 48 h from RILO-M1-G-contained G12 by examining FITC-tagged G12" is ambiguous. Please modify and confirm the usage of "RILO-M1-G-contained".

9. In Fig. 5a, the "tumor" should be written as "tumour" considering the unified style of the manuscript.

10. The statistical analysis in Supplementary Fig. 23 should be supplemented.

Reviewer #4 (Remarks to the Author):

In Liu, et. al., the authors describe in great detail the formulation and validation of lipid nanoparticle therapeutic that is packaged into M1 polarized macrophages. These macrophages, termed RILO-M1-G, were injected into mice, then deliver an inflammatory TLR7/8 agonist and an IDO1 inhibitor upon entry to tumors. This topic is of potential high biomedical significance as cell based therapies with efficacy against solid tumors are needed, and recently, concerns CART cell therapy associated malignancies have been identified as challenges with cell therapies capable of clonal expansion.

Significantly, the authors deeply the described cell therapy was efficacious promoting clearance of the H22 HCC tumor injection model, even in the absence of CD8 and CD4 T cells. This effect was linked to improved phagocytic clearance of tumor cells through in vitro experiments. On a cellular level, in vivo assays indicated that the RILO-M1-G cell therapy promoted heightened intertumor inflammation, heightened effector CD4 T cells and IFNgamma competenent CD8 T cell phenotype, reduced tumoral T regulatory cells, and augmented the M1 macrophage to M2 macrophage ratio. This model was also capabel of protecting mice from subsequent rechallenge with H22 cells, indicating improved adapive immune cell memory. Further, this model was equally efficacious against the H22 tumoral models when the cells were implanted orthotopically. And it is apparent

that consitutent component layers of the RILO-M1-G cell therapy are less efficacious alone, further hightlighting the value RILO-M1-G.

To their credit, the authors provied a very detailed manuscript, both in the results and methods sections. And shown experiments include necessary controls. However, this manuscript in the present form has several critical problems:
- The manuscript is very challenging to read. This is partly due to absent simplification of writing, selection of which data are necessary to support the conclusions, and which data are supportive but *unnecessary* internal validations.
- The manuscript may benefit from division into two seperate co-submitted articles, with the first article describing the chemistry and formulation of the macrophage drug deliver systems, and the second article describing the efficacy of the system in the preclinical models. This will also improve the quality of peer review because candidate referees will better be able to judge whether their own expertise is applicable. This is applicable on the part of this referee who lacks the expertise necessary to critically evaluate the chemistry of the nanoparticle/drug design aspects of the manuscript. These portions represented a majority of the article, which was not apparent from the abstract.
- Experimentally, there are also some critical unaddressed aspects which could heigten the significance of this manusript. The authors demosntrate that the RILO-M1-G cell therapy can be detected in multiple organs, including in the tumor. But it is unclear if the RILO-M1-G therapy cells account for the altered M1 to M2 ratio in vivo, or if the the action of the RILO-M1-G can directly convert tumor associated M2 macrophages into a beneficial M1 phenotype. In vitro evidence supports the direct action of RILO-M1-G on polarizing M2 cells towards the M1 phenotype.
- Last, and probably beyond the scope of this manuscript, it will be critical to validate this cell therapy, in an unrelated solid tumor model.

Minor concerns

- Line 164 refers to a different experiment than what is described in Figure 2b (text states R848 to INCB ratio; figure states ratio of M1 to M2 polarization)
- Are drugs being releases specifically in response to the target antigen? Is there an experiment demonstrating this?
- Figure 6b doesn't have units in the nor legend. Presumably they are pg/g as in SF17.
- There are some minor English issues throughout the manuscript.
- Panel sizes in figure 7g and SF24 are very small.

The Point-by-point Response to the Reviewers' Comments

Response to Reviewer 1 Comments:

The manuscript entitled as "On-demand editing macrophages enable specific phagocytosis and drug exosome generation for solid tumour cytotherapy" is a very original and well-conceived study. However, this study fails to prove an important point. Organization within a single figure(especially Fig. 2) makes it difficult to understand the content. In addition, the paper is riddled with inappropriate abbreviations (G12, DG12,RILO-M1-G, and RILO-M1-G (RAW264.7) ext.), and then that makes it difficult to understand. Authors would do well to organize the arrangement of the results.

Response: Thank you for your kind comments. We have reorganized the single figures (including Figures 2, 5, 6, 7 and 8) and improved the description of the corresponding figures to enhance the understanding of contents. In addition, the abbreviations involved in this manuscript have been rearranged. For example, G12 was changed to GTP to match its full English name "GPC3 targeting peptide". At the same time, we referred to the published references to distinguish the experiments results for macrophage-based formulations with BMDM or RAW264.7 using superscript form BMDM or RAW[1]. We hope these changes will meet the requirement. The revised description had been supplemented in the manuscript and marked in red in the revised manuscript.

Reference:

[1] Xu X, Wang Q, Qian X, Wu Y, Wang J, Li J, Li Y, Zhang Z. Spatial-Drug-Laden Protease-Activatable M1 Macrophage System Targets Lung Metastasis and Potentiates Antitumor Immunity. ACS Nano. 2023, 17, 5354-5372.

Major

1. Authors have not been able to prove that each compound (R848 or INCB) is contained in RILO. On Supplementary Table 1, it was measured the concentration of vesicles and compounds dissolving in the liquid. Authors shown the stability of vesicles in Supplementary Fig. 2, but how much of the compound remains in the vesicle?

Response: Thank you for your kind comments. According to the published references, 0.22 μm filter are often used to remove insoluble free drugs and filtration sterilization from lipid nanoparticles. For the high hydrophobicity drug, the amount of free drugs (un-encapsulated drugs)

remaining in the filtered lipid nanoparticles is very few, which generally considered to be negligible[1-3]. Both R848 and INCB are insoluble compound in water (high hydrophobicity drugs), the R848 and INCB that is not encapsulated into RILO will be precipitated when the water-soluble organic solvent (ethanol) used in the preparation process is completely removed, and these precipitated drugs unable to pass through the 0.22 μm filter and be removed. As described in the part of "methods", 0.22 μm filter was used to remove the free drugs to obtain RILO, and then the loading of R848 and INCB in RILO was quantified by HPLC after methanol demulsification. Therefore, the "DL of R848(%)" and "DL of INCB(%)" measured in "Supplementary Table 1" were the drug content in RILO.

Based on this method, we also added the storage stability of "DL of R848(%)" and "DL of INCB(%)", and the experimental results showed that RILO remained stable under storage conditions without substantial changes in particle size, zeta potential and DL of R848 and INCB for at least 14 days, respectively. The results were update and we hope these changes will meet the requirement. The revised description had been supplemented in the manuscript and marked in red in the revised manuscript.

Reference:

[1] Dosta P, Cryer AM, Dion MZ, Shiraishi T, Langston SP, Lok D, Wang J, Harrison S, Hatten T, Ganno ML, Appleman VA, Taboada GM, Puigmal N, Ferber S, Kalash S, Prado M, Rodríguez AL, Kamoun WS, Abu-Yousif AO, Artzi N. Investigation of the enhanced antitumour potency of STING agonist after conjugation to polymer nanoparticles. Nat Nanotechnol. 2023, 18, 1351-1363.

[2] Fu S, Chang L, Liu S, Gao T, Sang X, Zhang Z, Mu W, Liu X, Liang S, Yang H, Yang H, Ma Q, Liu Y, Zhang N. Temperature sensitive liposome based cancer nanomedicine enables tumour lymph node immune microenvironment remodelling. Nat Commun. 2023, 14, 2248.

[3] Hao M, Hou S, Li W, Li K, Xue L, Hu Q, Zhu L, Chen Y, Sun H, Ju C, Zhang C. Combination of metabolic intervention and T cell therapy enhances solid tumor immunotherapy. Sci Transl Med. 2020, 12, eaaz6667.

The revised parts were listed below:

RILO was stable in macrophages, and RILO@MG maintained the M1 phenotype in different culture environments.

The preparation of RILO@MG was mainly divided into two parts: the process of "inner packing"

by coincubating M1-type macrophages with RILO and the implementation of “surface anchoring” by inserting GTP into the lipid bilayers of the cell membrane via hydrophobic interactions, as illustrated in Fig. 2a. After a preliminary study, we determined that the mass ratio of R848 to INCB was between 6:5 and 6:6 (Supplementary Fig. 1), and the optimal concentration of C16-ceramide incubated with M1-type macrophages was 100 μM (Supplementary Fig. 2). Inspired by macrophages in naturally fighting bacteria and other pathogens[48, 49], we selected OMVs obtained from the culture medium of nonpathogenic *E. coli* MG1655 by multiple centrifugation and ultrafiltration steps as a component of RILO. The RIL was coextruded with C16-ceramide fused OMVs to prepare RILO. Transmission electron microscopy (TEM) images and dynamic light scattering analysis showed that RILO was approximately 50.54 nm in size with a core-shell-structured spherical morphology (Fig. 2b-d), indicating the successful assembly of RILO. R848 and INCB were efficiently loaded into RILO with drug loadings (DL, %) of 6.17±0.02% and 5.13±0.15% for R848 and INCB, respectively (Supplementary Table 1). Protein profiles in RILO were determined by SDS-polyacrylamide gel electrophoresis (SDS-PAGE), which confirmed that the proteins from the OMVs were retained in RILO (Fig. 2e). Moreover, RILO remained stable under storage conditions without substantial changes in particle size, zeta potential and DL of R848 and INCB for at least 14 days, respectively (Supplementary Fig. 3). RILO could also remain stable under physiological conditions during at least 48 hours (Supplementary Fig. 3). To mimic clinical settings, bone marrow-derived macrophages (BMDMs) were used in RILO@MG preparation unless marked RAW superscript. BMDMs were identified by morphology and flow cytometry (Supplementary Fig. 4).

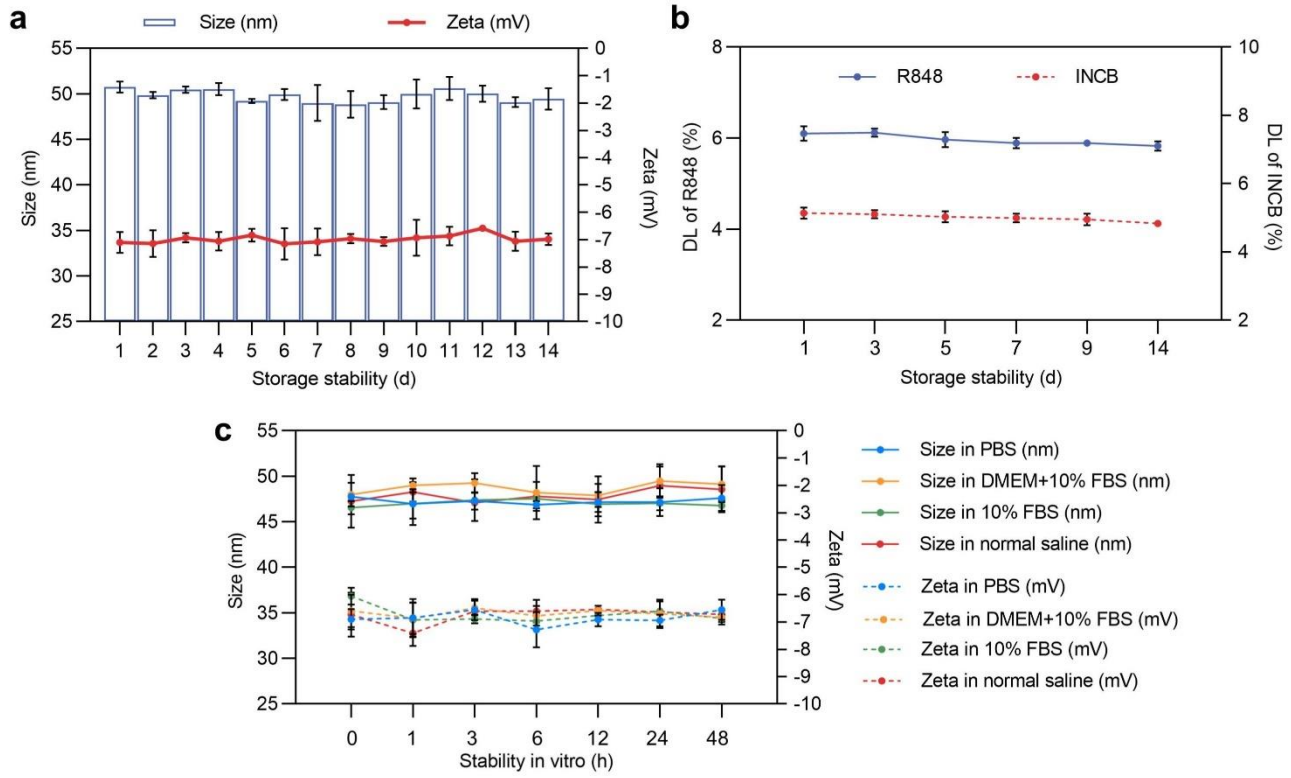

Supplementary Fig. 3. The stability of RILO under storage or physiological conditions. a, The changes of size and zeta potential of freshly prepared RILO with time after storage at 4 °C (n = 3 biologically independent experiments). b, The DL changes of R848 or INCB of freshly prepared RILO with time after storage at 4 °C (n = 3 biologically independent experiments). c, The size and zeta potential of RILO after incubation at PBS, DMEM contained 10% FBS, 10% FBS and normal saline at different time points (n = 3 biologically independent experiments). All data are shown as the mean ± SD.

2. The various names for macrophages in this paper are not very good. For example, M1-macrophage (RAW264.7), TAM, M2 macrophages, M1 in HCM etc. The results of RAW264.7 and bone marrow-derived macrophages should be organized.

Response: Thank you for your kind comments. According to your suggestion, we have improved the various names for macrophages in this manuscript. Based on the activation status and functions of macrophages, macrophages could be divided into M1 phenotype and M2 phenotype, so we uniformly named them M1-type macrophage and M2-type macrophage[1-2]. The injected formulations made by M1-type macrophages were designated as Blank@M, LO@MG, RILO@M, RILO@MG-, RILO+MG and RILO@MG, respectively. For macrophages infiltrated in tumor tissue, the published references mainly named them tumour-associated macrophages (TAM)[3]. For TAM model in vitro, it was mainly prepared by co-incubation of macrophages with tumor conditioned

medium, so the name TAM was also used in this manuscript[4].

In addition, we also referred to the published references to distinguish the experiments results for macrophage-based formulations with BMDM or RAW264.7 using superscript form BMDM or RAW[5]. We have marked "Bone marrow-derived macrophages (BMDMs) were used in all experiments involving macrophages unless marked RAW superscript" at appropriate places in the main text and figure legends. The corresponding experiment results for macrophage-based formulations using BMDM or RAW264.7 are summarized in the table below. We hope these changes will meet the requirement. The revised description had been supplemented in the manuscript and marked in red in the revised manuscript.

List of corresponding experiments results for macrophage-based formulations using BMDM or RAW264.7.

BMDM	RAW264.7
Fig. 2k-l, 3b-k, 4a-l, 5b-f, 5h, 5j, 5l-m, 6b-j, 7b-f, 7h, 7i and 8b-n	Fig. 2g-j
Supplementary Fig. 5b, 6, 8, 10b and 12-39	Supplementary Fig. 5a, 5c, 7, 8, 10a, 10c, 11
Supplementary Table 3	—

Reference:

[1] Germano G, Frapolli R, Belgiovine C, Anselmo A, Pesce S, Liguori M, Erba E, Uboldi S, Zucchetti M, Pasqualini F, Nebuloni M, van Rooijen N, Mortarini R, Beltrame L, Marchini S, Fuso Nerini I, Sanfilippo R, Casali PG, Pilotti S, Galmarini CM, Anichini A, Mantovani A, D'Incalci M, Allavena P. Role of macrophage targeting in the antitumor activity of trabectedin. Cancer Cell. 2013, 23, 249-262.

[2] Mosser DM, Edwards JP. Exploring the full spectrum of macrophage activation. Nat Rev Immunol. 2008, 8, 958-969.

[3] Wang X, Xu Y, Sun Q, Zhou X, Ma W, Wu J, Zhuang J, Sun C. New insights from the single-cell level: Tumor associated macrophages heterogeneity and personalized therapy. Biomed Pharmacother. 2022, 153, 113343.

[4] Lu CS, Shiau AL, Su BH, Hsu TS, Wang CT, Su YC, Tsai MS, Feng YH, Tseng YL, Yen YT, Wu CL, Shieh GS. Oct4 promotes M2 macrophage polarization through upregulation of

macrophage colony-stimulating factor in lung cancer. J Hematol Oncol. 2020, 13, 62.

[5] Xu X, Wang Q, Qian X, Wu Y, Wang J, Li J, Li Y, Zhang Z. Spatial-Drug-Laden Protease-Activatable M1 Macrophage System Targets Lung Metastasis and Potentiates Antitumor Immunity. ACS Nano. 2023, 17, 5354-5372.

3. The use of figure legend abbreviations should be reviewed.

Response: Thank you for your kind comments. According to your suggestion, the abbreviations involved in this manuscript have been reviewed. For example, G12 was changed to GTP to match its full English name "GPC3 targeting peptide". We have added "List of abbreviations" in the supporting information to make it easier for readers to understand. We hope these changes will meet the requirement. The revised description had been supplemented in the manuscript and marked in red in the revised manuscript.

The revised parts were listed below:

Supplementary Table 4. List of abbreviations.

Abbreviations	Dedinition
^{1}H-NMR	Proton nuclear magnetic resonance
ANOVA	Analysis of variance
BCA	Bicinchoninic acid
BMDM	Bone marrow-derived macrophage
C16-ceramide	Ceramide containing fatty acyl chains of 16 carbon atoms
C6	Coumarin-6
CAR	Chimeric antigen receptor
CAR-M	Chimeric antigen receptor macrophage
CCK-8	Cell counting kit-8
DL	Drug loading
E. coli	*Escherichia coli*
EE	Encapsulation efficiency
FBS	Foetal bovine serum
GPC3	Glypican-3
GTP	GPC3 targeting peptide
H&E	Haematoxylin and eosin

HCC	Hepatocellular carcinoma
HCM	HCC conditioned medium
HPLC	High-performance liquid chromatography
i.v.	Intravenous
IDO1	Indoleamine 2,3-dioxygenase 1
ILV	Intralumenal vesicle
INCB	INCB024360
Kyn	Kynurenine
M1-type macrophage^{RAW}	M1-type macrophages from RAW264.7 cell
M-CSF	Monocyte-colony stimulating factor
MST	Median survival time
MTT	Methylthiazolyldiphenyl-tetrazolium bromide
MVB	Multivesicular body
NS	Normal saline
OMV	Outer membrane vesicle
PDI	Polydispersity index
RI-exosome	R848/INCB024360-exosome
RIL	R848/INCB024360-lipid nanoparticle
RILO	R848/INCB024360-lipid outer membrane vesicle
RILO@M	RILO-packed M1-type macrophage
RILO@MG	GPC3 peptide-anchored RILO@M
RILO@MG-	RILO@MG without C16-ceramide
RILO+MG	Combination treatment of RILO and MG
RI-MV	R848/INCB024360-microvesicle
SDS-PAGE	SDS-polyacrylamide gel electrophoresis
TAM	Tumour-associated macrophage
TAM^{RAW}	TAM from RAW264.7 cell
TEM	Transmission electron microscopy
TLR	Toll-like receptor

TME	Tumour microenvironment
Treg	Regulatory T-cell
Trp	Tryptophan

Minor

4. Could TEM results be different from vesicles? For example, Fig. 2e and Fig. 3

Response: Thank you for your kind comments. Since both OMVs and exosomes are lipid vesicles containing a lot of protein components, they cannot be distinguished under TEM. Fig. 2e (equivalent to Fig. 2b in the revised manuscript) was the TEM image of RILO, which showed that RIL was successfully wrapped by OMV to form a core-shell-structured spherical morphology. Meanwhile, we also demonstrated the presence of OMV in RILO by SDS-polyacrylamide gel electrophoresis and label-free quantitative proteomics technology. The TEM image shown in Fig. 3 was mainly to prove that the released from RILO@MG still had nanostructures. As shown in the TEM results in Fig. 3h, we found that the released exosomes (nonfree drug form) from the RILO@MG group still had core-shell structure, and the shell was identified by western blotting as exosomes secreted by living macrophages.

Combined with dynamic light scattering analysis, we found that RILO was 50.54±0.40 nm in size and -7.44±0.31 mV in zeta potential (Supplementary Table 1), while RI-exosome released by RILO@MG was 87.57±4.21 nm in size and -8.77±0.28 mV in zeta potential (Supplementary Table 3), so there was a difference between the two. We hope these answers will meet the requirement.

Response to Reviewer 2 Comments:

This work with extensive experimental results has merit, and the following are recommended to be addressed in order to maximize its impact:

1. The whole text needs to be carefully reviewed for incomplete sentences, several of which were spotted across the manuscript.

Response: Thank you for your kind comments. We have reviewed the incomplete sentences in this manuscript. And the manuscript has been edited for proper English language, grammar, punctuation, spelling, and overall style by one or more of the highly qualified native English speaking editors at SNAS. The editing certificate has been listed below.

[CERTIFICATE REDACTED]

2. All the figure captions should be carefully reviewed to make sure that every panel has a caption and that the caption text and letter align with their panel.

Response: Thank you for your kind comments. We have carefully reviewed the figure captions in this manuscript according to the requirements of *Nature Communications*. Every panel has a caption and that the caption text and letter align with their panel in the revised manuscript.

3. It is unclear why the number of biological replicates for the in vivo experiments were varied (some n=3, others n=5 or n=6). Was there a statistical analysis done to determine how many replicates were needed for significance?

Response: Thank you for your kind comments. Thank you for your kind comments. The number of biological replicates for in vivo experiments were chosen according to the approval from the Laboratory Animal Ethical and Welfare Committee of Shandong University Cheeloo College of Medicine. The number of biological replicates was 5 or 6 in subcutaneous tumor model, which was considered acceptable for statistical analysis. And the number of biological replicates of 5 and 6 in the subcutaneous tumor model was also adopted in the references published by Nature Portfolio (Nat Commun, 2020, 11, 1126[1]; Nat Commun, 2023, 14, 3366[2]; Nat Commun, 2023, 14, 2950[3]; Nat Commun. 2022, 13, 7228[4]).

On the basis of the experimental results of subcutaneous tumor model, we used the orthotopic tumor model to conduct a revalidation study on the therapeutic effect, as shown in Fig. 8a. In the orthotopic H22 tumor model, the in vivo bioluminescence images and ex vivo livers of bioluminescence quantification were performed for 3 biological replicates. Following the "3R" principle of replacement, reduction and refinement[5], we used the resource equation approach to calculate the sample size of animals in each group[6]. The number of animals per group was calculated by the following equations: Min n = 10/K+1 and Max n = 20/K+1, where K = number of groups. Therefore, Min n = 2.67, Max n = 4.33. Based on the calculation results of the resource equation approach, we chose the number of biological replicates was 3. And the number of biological replicates of 3 in the orthotopic tumor model was also adopted in the references published by Nature Portfolio (Nat Nanotechnol, 2023, 18, 193-204[7]; Nat Commun, 2022, 13, 7772[8]; Nat Commun, 2020, 11, 446[9]).

In the orthotopic H22 tumor model, we used sophisticated instruments to detect tumor bioluminescence at no less than 5 time points for 20 consecutive days in each mouse, and bioluminescence was quantified for ex vivo livers. The standard deviation of different groups in this experiment was small enough to ensure that the influence of individual differences on the experimental results could be excluded. In addition, the results of the survival curve were again supported the experimental conclusion. From what has been discussed above, the biological replicates in this manuscript could meet the requirements of the statistical analysis, the obtained

conclusions were true and correct. We hope these replies will meet the requirement.

Reference:

[1] Li M, Li S, Zhou H, Tang X, Wu Y, Jiang W, Tian Z, Zhou X, Yang X, Wang Y. Chemotaxis-driven delivery of nano-pathogenoids for complete eradication of tumors post-phototherapy. Nat Commun. 2020, 11, 1126.

[2] Wang L, Wang G, Mao W, Chen Y, Rahman MM, Zhu C, Prisinzano PM, Kong B, Wang J, Lee LP, Wan Y. Bioinspired engineering of fusogen and targeting moiety equipped nanovesicles. Nat Commun. 2023, 14, 3366.

[3] Wang K, Li Y, Wang X, Zhang Z, Cao L, Fan X, Wan B, Liu F, Zhang X, He Z, Zhou Y, Wang D, Sun J, Chen X. Gas therapy potentiates aggregation-induced emission luminogen-based photoimmunotherapy of poorly immunogenic tumors through cGAS-STING pathway activation. Nat Commun. 2023, 14, 2950.

[4] Liu T, Li L, Wang S, Dong F, Zuo S, Song J, Wang X, Lu Q, Wang H, Zhang H, Cheng M, Liu X, He Z, Sun B, Sun J. Hybrid chalcogen bonds in prodrug nanoassemblies provides dual redox-responsivity in the tumor microenvironment. Nat Commun. 2022, 13, 7228.

[5] Percie du Sert N, Hurst V, Ahluwalia A, Alam S, Avey MT, Baker M, Browne WJ, Clark A, Cuthill IC, Dirnagl U, Emerson M, Garner P, Holgate ST, Howells DW, Karp NA, Lazic SE, Lidster K, MacCallum CJ, Macleod M, Pearl EJ, Petersen OH, Rawle F, Reynolds P, Rooney K, Sena ES, Silberberg SD, Steckler T, Würbel H. The ARRIVE guidelines 2.0: Updated guidelines for reporting animal research. PLoS Biol. 2020, 18, e3000410.

[6] Arifin WN, Zahiruddin WM. Sample Size Calculation in Animal Studies Using Resource Equation Approach. Malays J Med Sci. 2017, 24, 101-105.

[7] Chen Y, Huang Y, Li Q, Luo Z, Zhang Z, Huang H, Sun J, Zhang L, Sun R, Bain DJ, Conway JF, Lu B, Li S. Targeting Xkr8 via nanoparticle-mediated in situ co-delivery of siRNA and chemotherapy drugs for cancer immunochemotherapy. Nat Nanotechnol. 2023, 18, 193-204.

[8] Wang LC, Chang LC, Chen WQ, Chien YH, Chang PY, Pao CW, Liu YF, Sheu HS, Su WP, Yeh CH, Yeh CS. Atomically dispersed golds on degradable zero-valent copper nanocubes augment oxygen driven Fenton-like reaction for effective orthotopic tumor therapy. Nat Commun. 2022, 13, 7772.

[9] Wu L, Ishigaki Y, Hu Y, Sugimoto K, Zeng W, Harimoto T, Sun Y, He J, Suzuki T, Jiang X,

Chen HY, Ye D. H2S-activatable near-infrared afterglow luminescent probes for sensitive molecular imaging in vivo. Nat Commun. 2020, 11, 446.

4. It is unclear why statistical significance was processed using one-way ANOVA with Bonferroni correction -- this needs to be better justified, as the validity of the results hinges on this analysis being done properly.

Response: Thank you for your kind comments. When using one-way ANOVA for statistical analysis, the post hoc test is always required, and both Bonferroni's multiple comparisons test and Tukey's post hoc test are commonly used methods. We used GraphPad Prism 8 to conduct one-way ANOVA with Bonferroni's multiple comparisons test according to the published references[1-2].

Following your suggestions, we rechecked the statistical significance using one-way ANOVA analysis of variance with Tukey's post hoc test. We found that using either of the two methods had no effect on the conclusion of statistical significance involved this manuscript, so we used one-way ANOVA with Bonferroni's multiple comparisons test.

Reference:

[1] Sun X, Zhang Y, Li J, Park KS, Han K, Zhou X, Xu Y, Nam J, Xu J, Shi X, Wei L, Lei YL, Moon JJ. Amplifying STING activation by cyclic dinucleotide-manganese particles for local and systemic cancer metalloimmunotherapy. Nat Nanotechnol. 2021, 16, 1260-1270.

[2] Kellaway SG, Potluri S, Keane P, Blair HJ, Ames L, Worker A, Chin PS, Ptasinska A, Derevyanko PK, Adamo A, Coleman DJL, Khan N, Assi SA, Krippner-Heidenreich A, Raghavan M, Cockerill PN, Heidenreich O, Bonifer C. Leukemic stem cells activate lineage inappropriate signalling pathways to promote their growth. Nat Commun. 2024, 15, 1359.

5. It is a bit unclear how the results with this one particular cancer (HCC) and the proposed particular macrophage manipulation would translate into a broader application. The conclusion states that the components of RILOs and DG12 could "easily be incubated with isolated and purified autologous or allogeneic macrophages in vitro before patient use." Yet this methodology was not tested in this study with the mice.

Response: Thank you for your kind comments. For clinical trials, autologous or allogeneic human peripheral blood derived macrophages are commonly used cell types for macrophage-based cytotherapeutic. For preclinical studies, due to the small amount of blood collection allowed in mouse peripheral blood, bone marrow-derived macrophage has better homogeneity[1], and is often

used in the research related to macrophage-based cytotherapeutic, which has been recognized by many published references[2-4]. Therefore, in order to be more suitable for clinical transformation, we used bone marrow-derived macrophages to prepare RILO@MG for a series of evaluations such as in vivo antitumor activity.

To investigate a broader application of RILO@MG, in addition to the hepatocellular carcinoma-associated mouse model in the previous manuscript, we further verified the anti-tumour effects on B16F10 tumour-bearing mouse model with GPC3 expression[5-6]. The results were supplemented and we hope these changes will meet the requirement. The revised description had been supplemented in the manuscript and marked in red in the revised manuscript.

Reference:

[1] Zhao YL, Tian PX, Han F, Zheng J, Xia XX, Xue WJ, Ding XM, Ding CG. Comparison of the characteristics of macrophages derived from murine spleen, peritoneal cavity, and bone marrow. J Zhejiang Univ Sci B. 2017, 18, 1055-1063.

[2] Klichinsky M, Ruella M, Shestova O, Lu XM, Best A, Zeeman M, Schmierer M, Gabrusiewicz K, Anderson NR, Petty NE, Cummins KD, Shen F, Shan X, Veliz K, Blouch K, Yashiro-Ohtani Y, Kenderian SS, Kim MY, O'Connor RS, Wallace SR, Kozlowski MS, Marchione DM, Shestov M, Garcia BA, June CH, Gill S. Human chimeric antigen receptor macrophages for cancer immunotherapy. Nat Biotechnol. 2020, 38, 947-953.

[3] Shields CW 4th, Evans MA, Wang LL, Baugh N, Iyer S, Wu D, Zhao Z, Pusuluri A, Ukidve A, Pan DC, Mitragotri S. Cellular backpacks for macrophage immunotherapy. Sci Adv. 2020, 6, eaaz6579.

[4] Xu X, Wang Q, Qian X, Wu Y, Wang J, Li J, Li Y, Zhang Z. Spatial-Drug-Laden Protease-Activatable M1 Macrophage System Targets Lung Metastasis and Potentiates Antitumor Immunity. ACS Nano. 2023, 17, 5354-5372.

[5] Kandil D, Leiman G, Allegretta M, Evans M. Glypican-3 protein expression in primary and metastatic melanoma: a combined immunohistochemistry and immunocytochemistry study. Cancer. 2009, 117, 271-8.

[6] Motomura Y, Senju S, Nakatsura T, Matsuyoshi H, Hirata S, Monji M, Komori H, Fukuma D, Baba H, Nishimura Y. Embryonic stem cell-derived dendritic cells expressing glypican-3, a recently identified oncofetal antigen, induce protective immunity against highly metastatic mouse melanoma,

B16-F10. Cancer Res. 2006, 66, 2414-22.

The revised parts were listed below:

RILO@MG showed superb antitumour efficacy in an orthotopic HCC mouse model and B16F10 tumour-bearing mouse model.

To investigate the generalizability of RILO@MG, we further verified the anti-tumour effects on B16F10 tumour-bearing mouse model with GPC3 expression[53, 54]. The tumour photographs and tumour growth curves among different groups were shown in Fig. 8i and Supplementary Fig. 39a. After treatment, the tumour weight in RILO@MG group was only about 0.09 g, which was significantly lower than that in RILO@M group ($P < 0.001$), demonstrating the RILO@MG could inhibit the tumour progress (Fig. 8j, k). During the treatment, no significant difference was observed in the body weight changes, exhibiting the preliminary safety (Supplementary Fig. 39b). Similar to the H22 tumour-bearing mouse model, the RILO@MG group significantly enhanced intratumoural M1-type macrophages (Fig. 8l and Supplementary Fig. 39c), $CD4^+$ T cells (Fig. 8m), and $CD8^+$ T cells (Fig. 8n) infiltration, indicating that the immunomodulatory capacity of RILO@MG in the B16F10 tumour-bearing mouse model.

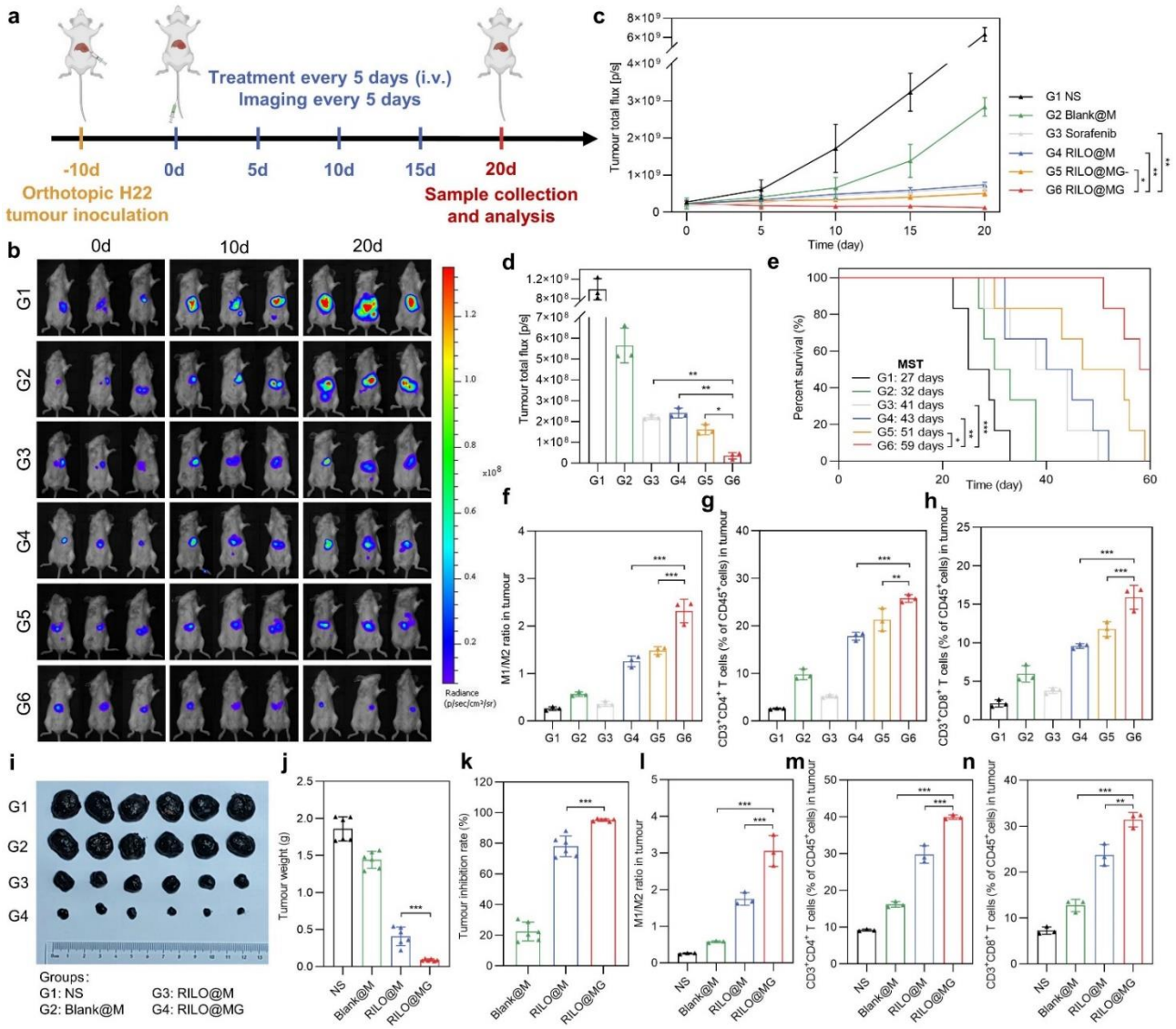

Fig. 8| Efficacy validation of RILO@MG in the orthotopic H22 tumour model and B16F10 tumour-bearing mouse model. a, Schematic of the orthotopic H22 tumour model experiment (dose of 3.0 × 10^6 cells per mouse per injection, equal to 4 mg/kg R848 and 3.4 mg/kg INCB; sorafenib: 10 mg/kg). **b-e,** In vivo bioluminescence images (**b**), bioluminescence intensity curves (**c**), ex vivo livers on Day 20 of bioluminescence quantification (**d**) and animal survival (**e**) of the orthotopic H22 tumour model receiving the indicated treatments (n = 3 biologically independent animals for **b-d** and n = 6 biologically independent animals for survival). **f-h,** Flow cytometry quantitative data of M1-type macrophage and M2-type macrophage (**f**) and $CD4^+$ and $CD8^+$ T cells (**g, h**) in tumours of mice sacrificed on Day 20 (n = 3 biologically independent animals). **i-k,** Tumour photographs (**i**), tumour weights (**j**) and tumour inhibition rate (**k**) of the sacrificed mice at the study endpoint (n = 6 biologically independent animals). **l-n,** Flow cytometry quantitative data of M1-type macrophage and M2-type macrophage (**l**) and $CD4^+$ and $CD8^+$ T cells (**m, n**) in tumours

of sacrificed mice (n = 3 biologically independent animals). Data are expressed as the mean ± SD. One-way ANOVA with Bonferroni's multiple comparisons test (**c, d, f-h**) and log-rank tests for survival data (**e**) were used for statistical analysis. *P < 0.05; **P < 0.01; ***P < 0.001. BMDMs were used in all experiments involving macrophages.

Response to Reviewer 3 Comments:

In this manuscript, Liu et al. developed innovative on-demand editing macrophages by incorporating surface glypican-3 (GPC3) peptide anchoring and inner lipid particle packing to effectively combat solid tumors. The ingenious modification of cells achieved effective phagocytosis and reversal of the tumor microenvironment, demonstrating both scientific significance and practical value. Particularly noteworthy was thediscovery that the membrane-modified targeting ligand on the surface of living macrophages could be transferred to extracellular vesicles,enabling tumor-targeted uptake and suggesting a novel mechanism for drug release from living cells. This study serves as an inspiration for thedevelopment of a new generation of macrophage-based cytotherapy. However, some issues needed to be addressed to further improve the manuscript before publication:

1. The GPC3 peptide G12 is the key ligand for the targeting action of macrophages in the manuscript. The authors suggested that GPC3 peptide G12 has superior specific targeting ability for H22 cells in the preliminary work. Please provide detailed discussion of the preliminary work andkey results related to the GPC3 peptide G12 in the “Introduction” or “Conclusions” section. Meanwhile, the application scope of G12 peptideneeds to be introduced.

Response: Thank you for your kind comments. GPC3 peptide G12 (G12 was called GTP in the revised manuscript) was selected based on the results of our previous studies[1]. We selected human hepatocarcinoma cell strains HepG2 and mouse hepatocarcinoma cell strains H22 as GPC3-positive cell models, whereas normal human liver cell strains HL-7702 and liverparenchymal cells as GPC3-negative cell models. The relative specific recognition ability of G7 (amino acid sequence: YFLTTAQ), G12 (amino acid sequence: DHLASLWWGTEL) and G14 (amino acid sequence: ALNVGGTYFLTTAQ) for GPC3-positive and GPC3-negative cells was evaluated via flow cytometer. Among them, G12 showed the highest specific recognition ability for HepG2 cells (64.24±6.49%) and H22 cells (55.54±6.47%). Therefore, G12 was a highly valuable targeting peptide for targeting tumors with GPC3 expression and was worthy of being used in the field of targeted drug delivery, such as hepatocellular carcinoma and melanoma. Based on these considerations, G12 was selected as the GPC3-targeting peptide in this manuscript. The revised description had been supplemented in the manuscript and marked in red in the revised manuscript.

Reference:

[1] Mu W, Jiang D, Mu S, Liang S, Liu Y, Zhang N. Promoting Early Diagnosis and Precise Therapy of Hepatocellular Carcinoma by Glypican-3-Targeted Synergistic Chemo-Photothermal Theranostics. ACS Appl Mater Interfaces. 2019, 11, 23591-23604.

The revised parts were listed below:

Discussion

Haematologic malignancies rapidly develop, and the efficacy of cytotherapy for the treatment of solid tumours has been difficult to enhance, which hinders the progress of this therapy in cancer treatment[8]. Considering the phagocytosis, specific targeting and deep penetration capacity of macrophages, macrophage-based cytotherapy has emerged. Clinical trials have provided evidence for the feasibility and safety of adoptively transferred macrophages[9]. Nevertheless, injected macrophages tend to change into the M2 phenotype in the immunosuppressive TME and lose immunological activity, resulting in poor transplantation efficacy, which is the key challenge to overcome to improve cytotherapy for the treatment of solid tumours. Here, we developed an on-demand editing macrophage, termed RILO@MG, obtained by surface GPC3 peptide anchoring and inner RILO packing to increase the immunological activity of injected macrophages.

According to our previous studies, the GTP with DHLASLWWGTEL amino acid sequence was selected, which showed the highest specific recognition ability for multiple tumor cells expressing GPC3[23]. We experimentally confirmed that RILO@MG released RI-exosomes and displayed excellent tumour accumulation and deep penetration capabilities by maintaining intact tumour chemotactic mobility and GPC3-mediated recognition. RILO@MG exerted immunotherapeutic effects primarily through three pathways, including the phagocytosis of tumour cells, regulation of the TAM phenotype and enhancement of T-cell activity, which jointly play a powerful antitumour immune role. Notably, administration of RILO@MG exerted remarkable antitumour efficacy in the rechallenged tumour model and tumour-bearing mouse model expressing GPC3 compared with that of all other experimental treatments. Compared with our previously reported nanoparticle-loaded macrophages, our current study focused on using surface anchoring and inner packing strategies to enhance the inherent function of M1-type macrophages in specifically killing tumours and remodelling the TME and emphasized the promotion of specific phagocytosis and drug exosome generation.

For on-demand editing of macrophages, the components of RILOs and DSPE-PEG_{5k}-GTP could

be industrially prepared and stably stored according to a standardized process and only need to be easily incubated with isolated and purified autologous or allogeneic macrophages in vitro before patient use. In conclusion, our proposed on-demand editing macrophage strategy bridges the gap between standardized and personalized treatment, shortens the waiting period for patients, and helps accelerate the commercialization of macrophage-based cytotherapy. In addition, the strategies presented here could be applied to other types of cells, such as dendritic cells and natural killer cells. As macrophages play crucial roles in various immune processes, the on-demand editing macrophages presented here may help in the treatment of other immune-related diseases.

2. Outer membrane vesicles (OMVs) from *Escherichia coli* were used for improving the drug loading of macrophage-based formulations. Please address safety concerns regarding the use of OMVs considering their bacterial origin.

Response: Thank you for your kind comments. OMVs are natural nanovesicles originating from Gram-negative bacteria. Due to numerous pathogen-associated molecular patterns, such as peptidoglycan, lipopolysaccharide and flagellin, the nanovesicles possess a potent capacity to activate innate immune signalling pathways[1-2]. Therefore, OMVs have been considered as vaccine adjuvants and vectors, but are not recommended for intravenous administration directly due to immunogenicity limitations. The OMV component used in this manuscript was coincubated with macrophages and loaded inside macrophages, which could avoid excessive immune response and even toxicity after intravenous injection. The experimental results showed that there was no body weight loss (Fig. 7e) or tissue damage (Supplementary Fig. 30) after RILO@MG treatment. Furthermore, RILO@MG did not cause the appearance of a cytokine storm after initial administration, which would be evident by elevated serum IL-6 and TNF-α levels (Supplementary Fig. 31), a significant change in the organ/body weight ratio at the study endpoint (Supplementary Fig. 32) and an increase in the levels of liver or kidney injury markers at the study endpoint (BUN, LDH, ALT, AST and ALP, Supplementary Fig. 33). These results confirmed that RILO@MG had preliminary safety in vivo.

Reference:

[1] Liu G, Ma N, Cheng K, Feng Q, Ma X, Yue Y, Li Y, Zhang T, Gao X, Liang J, Zhang L, Wang X, Ren Z, Fu YX, Zhao X, Nie G. Bacteria-derived nanovesicles enhance tumour vaccination by trained immunity. Nat Nanotechnol. 2023.

[2] Cheng K, Zhao R, Li Y, Qi Y, Wang Y, Zhang Y, Qin H, Qin Y, Chen L, Li C, Liang J, Li Y, Xu J, Han X, Anderson GJ, Shi J, Ren L, Zhao X, Nie G. Bioengineered bacteria-derived outer membrane vesicles as a versatile antigen display platform for tumor vaccination via Plug-and-Display technology. Nat Commun. 2021. 12, 2041.

3. In Fig. 2b and Supplementary Fig. 1, the TAM polarization effect was excellent when the mass ratio of R848 to INCB024360 was between 6:5and 6:6. Please confirm whether the ratio of R848 to INCB024360 remained between 6:5 and 6:6 upon release.

Response: Thank you for your kind comments. We calculated the cumulative release (μg) of R848 and INCB024360 at different time points during 72 h according to the data in Supplementary Fig. 12, and further calculated the ratio of cumulative release between R848 and INCB024360 at 1, 2, 4, 8, 12, 24, 48 and 72 h was 6:5.28, 6:5.88, 6:5.83, 6:5.78, 6:5.51, 6:5.41, 6:5.26 and 6:5.25, respectively. This proved that the ratio of R848 to INCB024360 remained between 6:5 and 6:6 upon release, which indicated an excellent TAM polarization effect.

4. In this manuscript, the authors made efforts to improve the treatment of hepatocellular carcinoma. However, the results in Fig. 4h showed that the accumulation of drugs in the liver was reduced compared with other groups. Please clarify the reason.

Response: Thank you for your kind comments. Glypican-3 could highly expressed at the tumor site of hepatocellular carcinoma patients, whereas it is not expressed in normal organs[1-3]. Due to the targeting ability of RILO@MG was GPC3-mediated, the drugs should accumulate more in the tumor expressing GPC3 site than that in other groups. Under the condition that the total amount of drugs in mice was the same, the accumulation of drugs in the tumor site of RILO@MG group was more, and the accumulation of drugs in normal liver site was less than that in other groups, which could be understood. This phenomenon could better support the conclusion of this manuscript: RILO@MG has strong tumour-directing abilities through chemotaxis and GPC3-mediated targeting action. We hope these replies will meet your requirement.

Reference:

[1] Mu W, Jiang D, Mu S, Liang S, Liu Y, Zhang N. Promoting Early Diagnosis and Precise Therapy of Hepatocellular Carcinoma by Glypican-3-Targeted Synergistic Chemo-Photothermal Theranostics. ACS Appl Mater Interfaces. 2019, 11, 23591-23604.

[2] Shih TC, Wang L, Wang HC, Wan YY. Glypican-3: A molecular marker for the detection and

treatment of hepatocellular carcinoma. Liver Res. 2020, 4, 168-172.

[3] Mu W, Chu Q, Yang H, Guan L, Fu S, Gao T, Sang X, Zhang Z, Liang S, Liu Y, Zhang N. Multipoint Costriking Nanodevice Eliminates Primary Tumor Cells and Associated-Circulating Tumor Cells for Enhancing Metastasis Inhibition and Therapeutic Effect on HCC. Adv Sci (Weinh). 2022, 9, 2101472.

5. As shown in the part of "3", it was mentioned that "compared with C6-LO and C6 released from LO-M1 groups, the fluorescence intensity of C6 released from LO-M1-G group showed no significant difference (Fig. 4c,d), which suggested that C6 released from LO-M1-G could be ingested by TAM as expected". Please explain the rationale for selecting the C6-LO group as the control for the LO-M1-G group.

Response: Thank you for your kind comments. It has been reported that outer membrane vesicles (OMVs) are easily recognized and phagocytized by macrophages because they possess numerous components from the parental bacterial outer membrane and periplasm[1-2]. According to the experimental results of this manuscript, the drug loading (μg/10^6) of RILO@M was 29.75±4.76 and 25.13±2.75 μg/10^6 for R848 and INCB, respectively, which was significantly higher than that of RIL@M (P < 0.001, Supplementary Fig. 8). It indicated the encapsulation of OMVs possessed higher internalization efficiency for M1-type macrophages than drug nanoparticles without OMV wrapping. Therefore, we selected the C6-LO group as the control for the LO-M1-G group.

Reference:

[1] Guo Q, Li X, Zhou W, Chu Y, Chen Q, Zhang Y, Li C, Chen H, Liu P, Zhao Z, Wang Y, Zhou Z, Luo Y, Li C, You H, Song H, Su B, Zhang T, Sun T, Jiang C. Sequentially Triggered Bacterial Outer Membrane Vesicles for Macrophage Metabolism Modulation and Tumor Metastasis Suppression. ACS Nano. 2021, 15, 13826-13838.

[2] Neupane AS, Willson M, Chojnacki AK, Vargas E Silva Castanheira F, Morehouse C, Carestia A, Keller AE, Peiseler M, DiGiandomenico A, Kelly MM, Amrein M, Jenne C, Thanabalasuriar A, Kubes P. Patrolling Alveolar Macrophages Conceal Bacteria from the Immune System to Maintain Homeostasis. Cell. 2020, 18, 110-125.e11.

6. Please provide insights into the source of macrophages when applying this strategy to human subjects.

Response: Thank you for your kind comments. This manuscript belongs to a preclinical study, bone

marrow-derived macrophage was used in macrophage-based formulation preparation. When applying this strategy to human subjects, autologous or allogeneic human peripheral blood derived macrophages[1] and induced pluripotent stem cell-derived macrophages[2-3] may be promising cell types for macrophage-based cytotherapeutic.

Reference:

[1] Klichinsky M, Ruella M, Shestova O, Lu XM, Best A, Zeeman M, Schmierer M, Gabrusiewicz K, Anderson NR, Petty NE, Cummins KD, Shen F, Shan X, Veliz K, Blouch K, Yashiro-Ohtani Y, Kenderian SS, Kim MY, O'Connor RS, Wallace SR, Kozlowski MS, Marchione DM, Shestov M, Garcia BA, June CH, Gill S. Human chimeric antigen receptor macrophages for cancer immunotherapy. Nat Biotechnol. 2020, 38, 947-953.

[2] Zhang L, Tian L, Dai X, Yu H, Wang J, Lei A, Zhu M, Xu J, Zhao W, Zhu Y, Sun Z, Zhang H, Hu Y, Wang Y, Xu Y, Church GM, Huang H, Weng Q, Zhang J. Pluripotent stem cell-derived CAR-macrophage cells with antigen-dependent anti-cancer cell functions. J Hematol Oncol. 2020. 13, 153.

[3] Lei A, Yu H, Lu S, Lu H, Ding X, Tan T, Zhang H, Zhu M, Tian L, Wang X, Su S, Xue D, Zhang S, Zhao W, Chen Y, Xie W, Zhang L, Zhu Y, Zhao J, Jiang W, Church G, Chan FK, Gao Z, Zhang J. A second-generation M1-polarized CAR macrophage with antitumor efficacy. Nat Immunol. 2024, 25, 102-116.

7. Please provide detailed methods for the screening process about the optimal concentration of C16-ceramide in Fig. 1c.

Response: Thank you for your kind comments. The detailed methods for the screening process about the optimal concentration of C16-ceramide were supplemented in the manuscript and marked in red in the revised manuscript.

The revised parts were listed below:

11 Formation and characterization of RI-exosomes. To observe the formation process of exosomes, Blank@M, RILO@MG- and RILO@MG were prepared. Six hours after preparation, Blank@M, RILO@MG- or RILO@MG were fixed with 2.5% glutaraldehyde aqueous solution, and the MVBs and ILVs were carefully imaged by TEM (HT7700, Hitachi, Tokyo, Japan).

To collect and purify the MVs and exosomes secreted by RILO@MG with serial centrifugation and ultracentrifugation following a previously reported protocol[57]. Briefly, freshly prepared RILO@MG was cultured in serum-free DMEM for 24 h. MVs were obtained by serial

centrifugation (300 × g for 10 min; 2,000 × g for 20 min and 16,500 × g for 30 min at 4 °C) of the cell culture medium. Exosomes were obtained by serial centrifugation (300 × g for 10 min; 2,000 × g for 20 min; 16,500 × g for 30 min and 120,000 × g for 90 min at 4 °C) of the cell culture medium. The MVs and exosomes secreted by Blank@M and RILO@MG- were prepared as described above. Exosomes were quantified by total protein concentration by BCA.

The size and zeta potential of exosomes were measured using a dynamic light scattering analyser. The morphology of exosomes stained with 1% phosphorus tungstate was observed by TEM. Exosome markers (CD63 and TSG101) were detected by western blotting. In brief, exosome protein extracts were isolated using RIPA buffer. Approximately 20 μg of exosome protein was loaded, subjected to fractionation by SDS-PAGE and transmembrane, and probed with anti-GAPDH, anti-CD63 or anti-TSG101 (Affinity Biosciences). Then, the signal was detected using an automatic chemiluminescence imaging analysis system (5200, Tanon, Shanghai, China).

To determine the optimal concentration of exosomes induced by C16-ceramide in M1-type macrophages, M1-type macrophages^{RAW} were treated with various concentrations of C16-ceramide (200, 100, 50, 25 or 0 μM) before the study began, released exosomes in 24 h were quantified by protein concentration (μg/10^6 cells).

8. As shown in the part of "3", the description of "we found that the RI-exosomes accumulated at 48 h from RILO-M1-G-contained G12 by examining FITC-tagged G12" is ambiguous. Please modify and confirm the usage of "RILO-M1-G-contained".

Response: Thank you for your kind comments. The usage of "RILO-M1-G-contained" has been revised. The revised description had been supplemented in the manuscript and marked in red in the revised manuscript.

The revised parts were listed below:

RILO@MG displayed excellent tumour accumulation and deep penetration capabilities.

The effect of RILO@MG on cellular uptake was evaluated in H22 cells and TAM^{RAW}. TAM^{RAW} were generated by culturing RAW264.7 cells in HCM for 24 h. Fluorescent-labelled C6 formulations were prepared. To elucidate drug uptake at the tumour site, C6 released cumulatively at 48 h from LO@M or LO@MG was collected for these experiments. For H22 cells, at 1 h and 4 h, the fluorescence intensity of C6 released from the LO@MG group was higher than that of C6 released from LO@M (Fig. 4a), and similar results were confirmed based on the data of flow cytometry ($P < 0.05$, $P < 0.01$, Fig. 4b). For TAM^{RAW}, the internalization of C6 released from LO@MG was time dependent. Compared with C6-LO and C6 released from LO@M groups, the

fluorescence intensity of C6 released from LO@MG group showed no significant difference (Fig. 4c,d), which suggested that C6 released from LO@MG could be ingested by TAM as expected. Furthermore, we found that the RI-exosomes accumulated at 48 h from RILO@MG contained GTP by examining FITC-tagged GTP (Supplementary Fig. 13). In the uptake experiments of these RI-exosomes by H22 cells, the fluorescence intensity of the C6-exosomes released from the LO@MG group was stronger than that of the C6-exosomes released from the LO@M group. The experimental results of the competitive inhibition assay showed that GPC3 mediated C6-exosome release from LO@MG into H22 cells rather than TAM^{RAW} (Supplementary Figs. 14 and 15). These results demonstrated that C6 released from LO@MG could be efficiently internalized into H22 cells and TAMs.

9. In Fig. 5a, the "tumor" should be written as "tumour" considering the unified style of the manuscript.

Response: Thank you for your kind comments. The Fig. 5a has been revised to form the unified style of the manuscript.

10. The statistical analysis in Supplementary Fig. 23 should be supplemented.

Response: Thank you for your kind comments. The statistical analysis in Supplementary Fig. 23 (equivalent to Supplementary Fig. 28 in the revised manuscript) has be supplemented. The revised description had been supplemented in the manuscript and marked in red in the revised manuscript.

The revised parts were listed below:

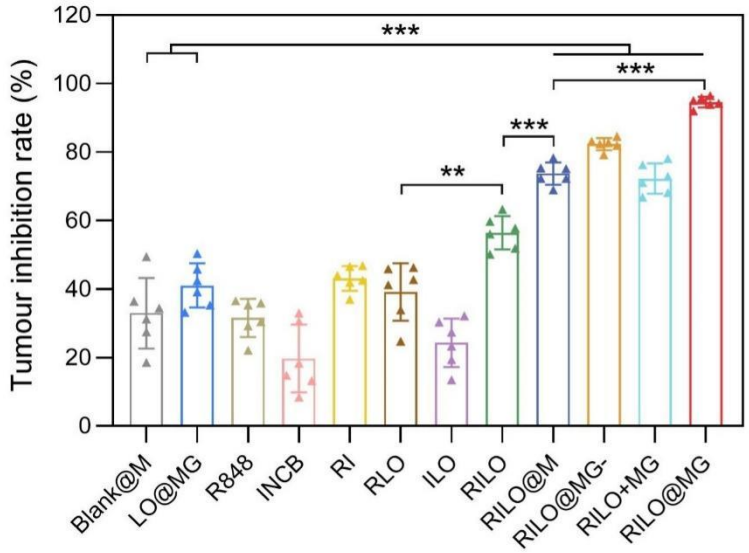

Supplementary Fig. 28. Tumour inhibition rate calculated based on Fig 7d. All data are shown

as the mean ± SD with $n = 6$ biologically independent animals. All data were analysed by one-way ANOVA with Bonferroni's multiple comparisons test. $^{**}P < 0.01$; $^{***}P < 0.001$.

Response to Reviewer 4 Comments:

In Liu, et. al., the authors describe in great detail the formulation and validation of lipid nanoparticle therapeutic that is packaged into M1 polarized macrophages. These macrophages, termed RILO-M1-G, were injected into mice, then deliver an inflammatory TLR7/8 agonist and an IDO1 inhibitor upon entry to tumors. This topic is of potential high biomedical significance as cell based therapies with efficacy against solid tumors are needed, and recently, concerns CAR-T cell therapy associated malignancies have been identified as challenges with cell therapies capable of clonal expansion.

Significantly, the authors deeply the described cell therapy was efficacious promoting clearance of the H22 HCC tumor injection model, even inthe absence of CD8 and CD4 T cells. This effect was linked to improved phagocytic clearance of tumor cells through in vitro experiments. On a cellular level, in vivo assays indicated that the RILO-M1-G cell therapy promoted heightened intertumor inflammation, heightened effector CD4 Tcells and IFNgamma competenent CD8 T cell phenotype, reduced tumoral T regulatory cells, and augmented the M1 macrophage to M2macrophage ratio. This model was also capabel of protecting mice from subsequent rechallenge with H22 cells, indicating improved adapiveimmune cell memory. Further, this model was equally efficacious against the H22 tumoral models when the cells were implanted orthotopically.And it is apparent that consitutent component layers of the RILO-M1-G cell therapy are less efficacious alone, further hightlighting the valueRILO-M1-G.

To their credit, the authors provied a very detailed manuscript, both in the results and methods sections. And shown experiments includenecessary controls. However, this manuscript in the present form has several critical problems:

1. The manuscript is very challenging to read. This is partly due to absent simplification of writing, selection of which data are necessary to support the conclusions, and which data are supportive but *unnecessary* internal validations.

Response: Thank you for your kind comments. We have reorganized the single figures (including Figures 2, 5, 6, 7 and 8), removed supportive but unnecessary data and improved the description of the corresponding figures to enhance the understanding of contents. The revised description had been refined in the manuscript and marked in red in the revised manuscript. We hope these changes will meet your requirement.

2. The manuscript may benefit from division into two seperate co-submitted articles, with the first article describing the chemistry and formulation of the macrophage drug deliver systems, and the second article describing the efficacy of the system in the preclinical models. This will also improve the quality of peer review because candidate referees will better be able to judge whether their own expertise is applicable. This is applicable on the part of this referee who lacks the expertise necessary to critically evaluate the chemistry of the nanoparticle/drug design aspects of the manuscript. These portions represented a majority of the article, which was not apparent from the abstract.

Response: Thank you for your kind comments. For better maintain the integrity of the design, the formulation of the macrophage drug deliver system and its efficacy in the preclinical models were integrated in one manuscript. Furthermore, according to the information displayed on the review interface, there are four reviewers for the peer-review from four different fields including "Bacterial OMV-macrophage interaction", "Macrophages/Cancer Immunotherapy/Drug Delivery", "Macrophages/Cancer Immunotherapy/HCC" and "Immune TME/Therapy/Macrophages", which is able to guarantee the quality of this manuscript. And all the reviewers have provided comprehensive and professional guidance. According this these valuable advises and suggestions, we have also revised the abstract, key words, introduction and discussion. We hope these changes will meet your requirement.

3. Experimentally, there are also some critical unaddressed aspects which could heigten the significance of this manusript. The authors demosntrate that the RILO-M1-G cell therapy can be detected in multiple organs, including in the tumor. But it is unclear if the RILO-M1-G therapy cells account for the altered M1 to M2 ratio in vivo, or if the the action of the RILO-M1-G can directly convert tumor associated M2 macrophages into a beneficial M1 phenotype. In vitro evidence supports the direct action of RILO-M1-G on polarizing M2 cells towards the M1phenotype.

Response: Thank you for your kind comments. After injecting RILO@MG, the intratumoural macrophage contained adoptively transferred macrophage and endogenous tumor-associated macrophage (TAM). In order to explore the action of RILO@MG about converting TAM into a beneficial M1 phenotype, we distinguished adoptively transferred macrophage and TAM by fluorescent labeling technology[1]. We used IVISense 680 fluorescent dye labeling injected macrophage of Blank@M, RILO@M and RILO@MG groups to evaluate the phenotypes of

adoptively transferred macrophage and TAM in an H22 tumour-bearing mouse model. The experimental results were supplemented and we hope these changes will meet the requirement. The revised description had been supplemented in the manuscript and marked in red in the revised manuscript.

Reference:

[1] Shields CW 4th, Evans MA, Wang LL, Baugh N, Iyer S, Wu D, Zhao Z, Pusuluri A, Ukidve A, Pan DC, Mitragotri S. Cellular backpacks for macrophage immunotherapy. Sci Adv. 2020, 6, eaaz6579.

The revised parts were listed below:

RILO@MG played an immunotherapeutic role by specifically phagocytizing tumour cells, regulating the TAM phenotype and reducing the percentage of Kyn/Trp.

Theoretically, highly activated M1-type macrophages could reverse the phenotype of adjacent M2-type macrophages by secreting cytokines, exosomes and other mechanisms. In our study, RI-exosomes generated from RILO@MG could further enhance M2-to-M1 reversion. TAMs were provided by culturing BMDMs in HCM for 24 h. We explored the influence of RILO@MG on TAMs by continuing to coincubate the two kinds of cells in HCM in Transwell plates (pore size 0.4 μm). The TAMs incubated in the lower chamber were collected for flow cytometry. Based on the calculation of the M1/M2 ratio (Fig. 5h and Supplementary Fig. 17), it was found that the ratio of freshly harvested TAMs dropped from 0.89±0.15 to 0.52±0.02 after continuing culture in HCM for 24 h when the upper chamber was free of formulations. In contrast, the calculation of the M1/M2 ratio was elevated sharply to 1.57±0.15 when RILO@MG was introduced in coculture for 24 h, which showed a higher ratio than that of the RILO@MG- group ($P < 0.05$), indicating that releasing drugs in exosome form exerted an excellent effect on the M2-to-M1 reversion of TAM in the lower chamber. Adoptively transferred macrophage and TAM in the tumour could be distinguished by fluorescent labeling technology[13]. Based on this, we used IVISense 680 fluorescent dye labeling injected macrophage of Blank@M, RILO@M and RILO@MG groups to evaluate the phenotypes of adoptively transferred macrophage and TAM in an H22 tumour-bearing mouse model (Supplementary Fig. 18). We found that RILO@M and RILO@MG could maintain the M1 phenotype in vivo. And the experiment results furtherly showed that endogenous TAM of mice treated with RILO@MG were polarized to M1 phenotype, as evidenced by significantly increased

expressions of CD80 compared with TAM of mice treated with Blank@M ($P < 0.001$), which indicated the action of RILO@MG could convert TAM to play anti-tumour role.

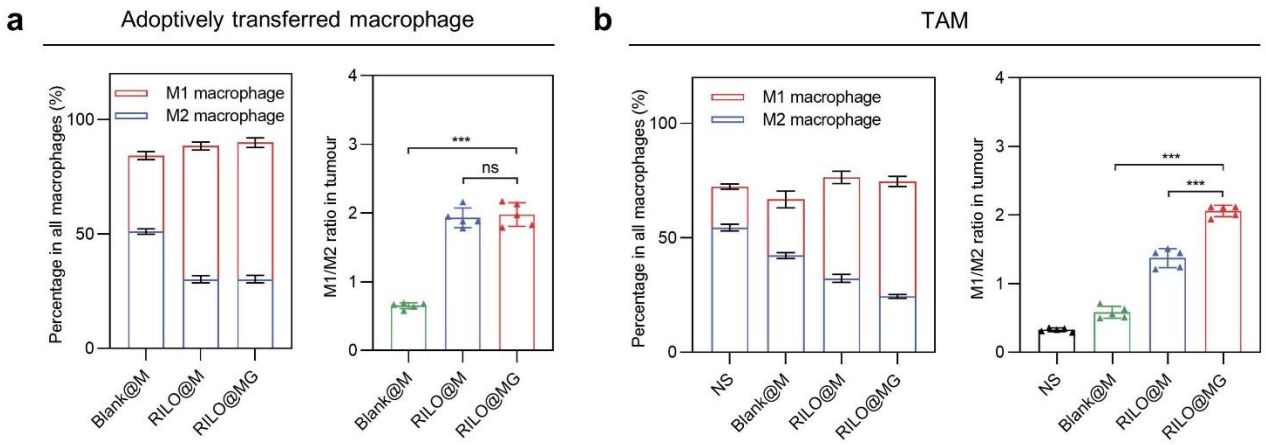

Supplementary Fig. 18. The phenotype analysis of adoptively transferred macrophage and TAM after injection. Mice inoculated with H22 cells were treated with adoptively transferred macrophage labeled with IVISense 680 fluorescent cell labeling dye. The intratumoural macrophage contained adoptively transferred macrophage and endogenous TAM, and the adoptively transferred macrophage could be distinguished by a flow cytometer. **a,** The phenotype analysis of adoptively transferred macrophage after i.v. administration with different formulations based on macrophages (n = 5 biologically independent animals). **b,** The phenotype analysis of endogenous TAM after injection of groups related to **a** (n = 5 biologically independent animals). All data are shown as the mean ± SD and were analysed by one-way ANOVA with Bonferroni's multiple comparisons test. ***$P < 0.001$; ns, no significance.

4. Last, and probably beyond the scope of this manuscript, it will be critical to validate this cell therapy, in an unrelated solid tumor model.

Response: Thank you for your kind comments. To investigate a broader application of RILO@MG, we validated the antitumor effect of RILO@MG in an unrelated solid tumor model. In addition to the hepatocellular carcinoma-associated mouse model in the previous manuscript, we further verified the anti-tumour effects on B16F10 tumour-bearing mouse model with GPC3 expression[1-2]. The results were supplemented and we hope these changes will meet the requirement. The revised description had been supplemented in the manuscript and marked in red in the revised manuscript.

Reference:

[1] Kandil D, Leiman G, Allegretta M, Evans M. Glypican-3 protein expression in primary and

metastatic melanoma: a combined immunohistochemistry and immunocytochemistry study. Cancer. 2009, 117, 271-8.

[2] Motomura Y, Senju S, Nakatsura T, Matsuyoshi H, Hirata S, Monji M, Komori H, Fukuma D, Baba H, Nishimura Y. Embryonic stem cell-derived dendritic cells expressing glypican-3, a recently identified oncofetal antigen, induce protective immunity against highly metastatic mouse melanoma, B16-F10. Cancer Res. 2006, 66, 2414-22.

The revised parts were listed below:

RILO@MG showed superb antitumour efficacy in an orthotopic HCC mouse model and B16F10 tumour-bearing mouse model.

To investigate the generalizability of RILO@MG, we further verified the anti-tumour effects on B16F10 tumour-bearing mouse model with GPC3 expression[53, 54]. The tumour photographs and tumour growth curves among different groups were shown in Fig. 8i and Supplementary Fig. 39a. After treatment, the tumour weight in RILO@MG group was only about 0.09 g, which was significantly lower than that in RILO@M group ($P < 0.001$), demonstrating the RILO@MG could inhibit the tumour progress (Fig. 8j, k). During the treatment, no significant difference was observed in the body weight changes, exhibiting the preliminary safety (Supplementary Fig. 39b). Similar to the H22 tumour-bearing mouse model, the RILO@MG group significantly enhanced intratumoural M1-type macrophages (Fig. 8l and Supplementary Fig. 39c), $CD4^+$ T cells (Fig. 8m), and $CD8^+$ T cells (Fig. 8n) infiltration, indicating that the immunomodulatory capacity of RILO@MG in the B16F10 tumour-bearing mouse model.

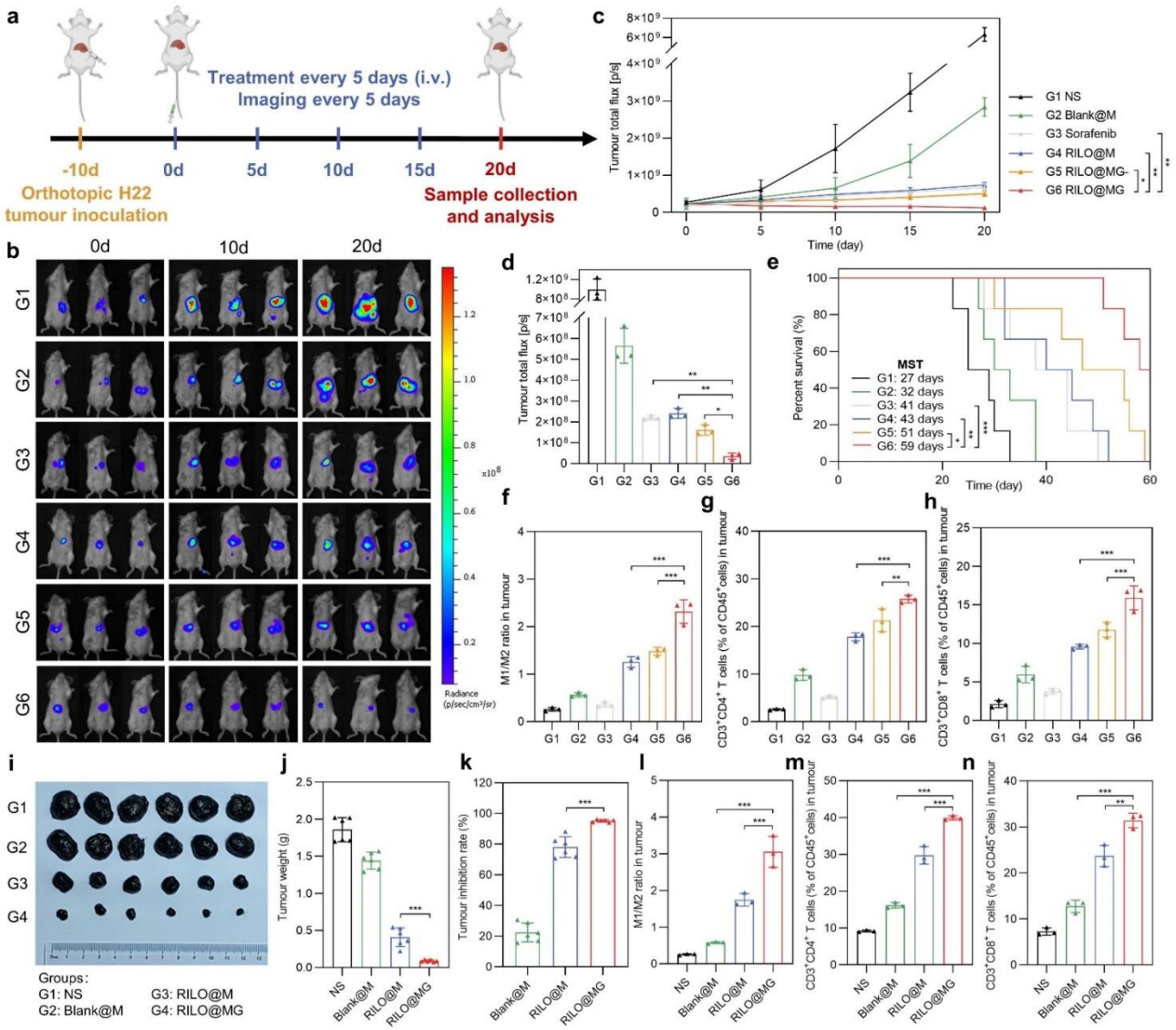

Fig. 8| Efficacy validation of RILO@MG in the orthotopic H22 tumour model and B16F10 tumour-bearing mouse model. a, Schematic of the orthotopic H22 tumour model experiment (dose of 3.0 × 10^6 cells per mouse per injection, equal to 4 mg/kg R848 and 3.4 mg/kg INCB; sorafenib: 10 mg/kg). **b-e,** In vivo bioluminescence images (**b**), bioluminescence intensity curves (**c**), ex vivo livers on Day 20 of bioluminescence quantification (**d**) and animal survival (**e**) of the orthotopic H22 tumour model receiving the indicated treatments (n = 3 biologically independent animals for **b-d** and n = 6 biologically independent animals for survival). **f-h,** Flow cytometry quantitative data of M1-type macrophage and M2-type macrophage (**f**) and $CD4^+$ and $CD8^+$ T cells (**g, h**) in tumours of mice sacrificed on Day 20 (n = 3 biologically independent animals). **i-k,** Tumour photographs (**i**), tumour weights (**j**) and tumour inhibition rate (**k**) of the sacrificed mice at the study endpoint (n = 6 biologically independent animals). **l-n,** Flow cytometry quantitative data of M1-type macrophage and M2-type macrophage (**l**) and $CD4^+$ and $CD8^+$ T cells (**m, n**) in tumours

of sacrificed mice (n = 3 biologically independent animals). Data are expressed as the mean ± SD. One-way ANOVA with Bonferroni's multiple comparisons test (**c, d, f-h**) and log-rank tests for survival data (**e**) were used for statistical analysis. *P < 0.05; **P < 0.01; ***P < 0.001. BMDMs were used in all experiments involving macrophages.

Minor concerns

5. Line 164 refers to a different experiment than what is described in Figure 2b (text states R848 to INCB ratio; figure states ratio of M1 to M2 polarization).

Response: Thank you for your kind comments. Figure 2b showed the changes in M1/M2 ratio at the different mass ratio of R848 to INCB. According to the changes in M1/M2 ratio, we determined that the mass ratio of R848 to INCB was between 6:5 and 6:6. The states were revised and we hope these changes will meet the requirement. The revised description had been supplemented in the manuscript and marked in red in the revised manuscript.

The revised parts were listed below:

RILO was stable in macrophages, and RILO@MG maintained the M1 phenotype in different culture environments.

The preparation of RILO@MG was mainly divided into two parts: the process of "inner packing" by coincubating M1-type macrophages with RILO and the implementation of "surface anchoring" by inserting GTP into the lipid bilayers of the cell membrane via hydrophobic interactions, as illustrated in Fig. 2a. We determined that the mass ratio of R848 to INCB was between 6:5 and 6:6 according to the changes in M1/M2 ratio (Supplementary Fig. 1), and the optimal concentration of C16-ceramide incubated with M1-type macrophages was 100 μM (Supplementary Fig. 2).

6. Are drugs being releases specifically in response to the target antigen? Is there an experiment demonstrating this?

Response: Thank you for your kind comments. In terms of drug release, our design was mainly to regulate the release form of the drug loaded in the macrophage, rather than the specific release in response to the target antigen. The experimental results suggested that RILO@MG could release loaded drugs in exosome form. Currently, the living cytopharmaceuticals releasing drugs in response to the target antigen were mainly loaded with drugs on the cell surface[1]. With the development of technology, we look forward to more discussions on the feasibility of antigen-responsive release of intracellular loaded living cytopharmaceuticals.

Reference:

[1] Chen Y, Chen X, Bao W, Liu G, Wei W, Ping Y. An oncolytic virus-T cell chimera for cancer immunotherapy. Nat Biotechnol. 2024.

7. Figure 6b doesn't have units in the nor legend. Presumably they are pg/g as in SF17.

Response: Thank you for your kind comments. We have added the corresponding units in Fig. 6b.

8. There are some minor English issues throughout the manuscript.

Response: Thank you for your kind comments. We have reviewed the minor English issues in this manuscript. And the manuscript has been edited for proper English language, grammar, punctuation, spelling, and overall style by one or more of the highly qualified native English speaking editors at SNAS. The editing certificate has been listed below.

[CERTIFICATE REDACTED]

9. Panel sizes in figure 7g and SF24 are very small.

Response: Thank you for your kind comments. We have modified the panel sizes in Figure 7g (equivalent to Supplementary Fig. 29 in the revised manuscript) and SF24 (equivalent to Supplementary Fig. 30 in the revised manuscript).

REVIEWER COMMENTS

Reviewer #1 (Remarks to the Author):

The manuscript entitled as "On-demand editing macrophages enable specific phagocytosis and drug exosome generation for solid tumour cytotherapy" is very unique as it proposes to use exosomes from macrophages as tumor suppressor. In introduction, many references are not appropriate. They are not consistent with the content. Authors need to read the references again.

Major
1. In feference 9, it was not shown that macrophage's circulation time is limited, and macrophages lead to lower off-target toxicity.
2. What is h on lane 62? If h means M1-type macrophages, reference 16 did not propose M1-type macrophages can downregulate the expression of SIRPα.
3. References 18–19 did not show that M1-type macrophages phagocytose tumor cells.
4. References 44 and 45 did not shown that FimH of E. coli and OMV interacts with caveolae of macrophages.

Reviewer #2 (Remarks to the Author):

Thank you for addressing the reviewers' feedback. The addition of B16F10 data to Fig. 8 is informative. However, the figure should be reworked to coherently incorporate these additional data:
- The schematic and caption for Panel (a) should mention H22 or B16F10.
- Panels f-h should be labeled in the figure and the caption should refer to H22.
- Panels i-j should be labeled in the figure and the caption should refer to B16F10.
- Panels m and n need to be mentioned in the caption (and refer to B16F10).

Reviewer #3 (Remarks to the Author):

Accept

Reviewer #4 (Remarks to the Author):

In Liu et. al, the authors describe a formulation and potential mechanism of action for an innovative cytotherapy strategy. They show through a directed design strategy that the cytotherapy alters the function of macrophages, protects mice from preclinical tumor models, and may lead to enhanced tumor specific T cell responses.

My major concern is the manuscript lacks organization and is overwhelmingly dense. This opinion was partially reflected in Reviewer 1's assessment. Although the authors did eliminate some primary figure panels, the supplement was expanded to 39 figures. A key recommendation was to simplify the study by focusing on necessary data. One intent was reflection on study designs and necessary control groups in order to simplify description of RILO@MG effects. Simplification could greatly improve reader appreciation of their findings. For example, some experiments in figures 6 and 7 include 13 groups. This is concerning because the authors do not provide rationale or context to their study design, or justify why at times the groupwise differences are inconsistent. It is not adequate to state that the RILO@MG group is different from a group. Related, this may point to a statistical concern on multiple hypothesis testing. Although the authors provide Bonferroni post-hoc p-values for One-Way ANOVA assessments, they never indicate if the overall ANOVA p-

values meet significance criteria to pursue post-hoc tests. Indeed, rebuttal statements to reviewer 2 may reflect some basic misunderstanding on ANOVA and attributes of chosen post-hoc tests. In this regard, several experiments misuse ANOVA based on the statistical assumptions or normal distribution and independent samples (eg. 8k, 7b, 7i)

My opinion stands that the relative impact of this study may be improved by splitting it into two parts: one part describing results with "formulating the macrophage drug deliver(sic) system"; the second part evaluating the "efficacy in the preclinical models." Sections valuating efficacy in the preclinical models are lacking in design, development, and rationale. Although evidence is generally supportive, the relevant aspects in the results and discussion are not well developed. This concern may be true for the drug design aspects as well.

Although the premise remains interesting and of potentially high biomedical significance, there are critical weaknesses remaining. My overall impression is the impact of the manuscript will be limited by presentation style.

The Point-by-point Response to the Reviewers' Comments

Response to Reviewer 1 Comments:

The manuscript entitled as "On-demand editing macrophages enable specific phagocytosis and drug exosome generation for solid tumour cytotherapy" is very unique as it proposes to use exosomes from macrophages as tumor suppressor. In introduction, many references are not appropriate. They are not consistent with the content. Authors need to read the references again.

Major

1. In reference 9, it was not shown that macrophage's circulation time is limited, and macrophages lead to lower off-target toxicity.

Response: Thank you for your kind comments. We had updated the reference 9 and the updated reference mentioned that "in terms of safety, macrophages have a low risk of graft-versus-host disease with a limited time in circulation and less non-tumor toxicity"[1]. We hope these changes will meet the requirement. The updated reference 9 had been supplemented in the manuscript and marked in red in the revised manuscript.

Reference:

[1] Shen J, Lyu S, Xu Y, Zhang S, Li L, Li J, Mou J, Xie L, Tang K, Wen W, Peng X, Yang Y, Shi Y, Li X, Wang M, Li X, Wang J, Cheng T. Activating innate immune responses repolarizes hPSC-derived CAR macrophages to improve anti-tumor activity. Cell Stem Cell. 2024, 31, 1-17.

The revised parts were listed below:

Moreover, macrophages lead to lower off-target toxicity due to their limited circulation time, and a large number of clinical trials have demonstrated the feasibility and safety of adoptively transferred macrophages[9, 10].

2. What is h on lane 62? If h means M1-type macrophages, reference 16 did not propose M1-type macrophages can downregulate the expression of SIRPα.

Response: Thank you for your kind comments. The h meant M1-type macrophages, which had

been corrected. We had updated the reference 16 and the updated reference mentioned that "compared with proinflammatory M1 macro-phages, the immunosuppressive M2 macrophages display amuch higher expression level of SIRPα" [1]. We hope these changes will meet the requirement. The updated reference 16 had been supplemented in the manuscript and marked in red in the revised manuscript.

Reference:

[1] Wei Y, Zhao M, He T, Chen N, Rao L, Chen L, Zhang Y, Yang Y, Yuan Q. Quantitatively Lighting up the Spatial Organization of CD47/SIRPα Immune Checkpoints on the Cellular Membrane with Single-Molecule Localization Microscopy. ACS Nano. 2023, 17, 21626-21638.

The revised parts were listed below:

Compared with M2-type macrophages, M1-type macrophages can downregulate the expression of SIRPα[16, 17] and have a stronger ability to directly phagocytose tumour cells, release cytokines and continuously activate downstream adaptive immune responses[18-21].

3. References 18-19 did not show that M1-type macrophages phagocytose tumor cells.

Response: Thank you for your kind comments. We had updated the references 18-19 and the updated references mentioned that "Proinflammatory M1 macrophages can phagocytose tumor cells, while antiinflammatory M2 macrophages such as tumor-associated macrophages (TAMs) promote tumor growth and invasion"[1] and "taken together, these results show that concurrent knock-down of SIRPα and CSF1-R can repolarize macrophages from the protumorigenic M2 to an antitumorigenic M1 phenotype and increase the phagocytosis effect of macrophages". We hope these changes will meet the requirement. The updated references 18-19 had been supplemented in the manuscript and marked in red in the revised manuscript.

Reference:

[1] Xia Y, Rao L, Yao H, Wang Z, Ning P, Chen X. Engineering Macrophages for Cancer Immunotherapy and Drug Delivery. Adv Mater. 2020, 32, e2002054.

[2] Zhao C, Cheng Y, Huang P, Wang C, Wang W, Wang M, Shan W, Deng H. X-ray-Guided In Situ Genetic Engineering of Macrophages for Sustained Cancer Immunotherapy. Adv Mater. 2023, 35, e2208059.

The revised parts were listed below:

Compared with M2-type macrophages, M1-type macrophages can downregulate the expression of

SIRPα[16, 17] and have a stronger ability to directly phagocytose tumour cells, release cytokines and continuously activate downstream adaptive immune responses[18-21].

4. References 44 and 45 did not shown that FimH of E. coli and OMV interacts with caveolae of macrophages.

Response: Thank you for your kind comments. We read references 44 and 45 carefully again. The reference 44 mentioned that "FimH-expressing *E.coli* can induce uptake by both mast cells and macrophages via an endocytic route that is distinct from the classical endosome-lysosome pathway and as a result, the bacteria remain in a viable state within morphologically distinct intracellular compartments" and depicted "model depicting bacteria-induced mobilization of caveolae"[1], and the reference 45 mentioned that "We propose that non-opsonized FimH-expressing *E. coli* co-opt internalization of lipid-rich microdomains following binding to the FimH receptor, the glycosylphosphatidylinositol-linked protein CD48, because (1) the sterol-binding agents filipin, nystatin and methyl b-cyclodextrin specifically block FimH-mediated internalization; (2) CD48 and the protein caveolin both accumulate on macrophage membranes surrounding bacteria; and (3) antibodies against CD48 inhibit FimH-mediated internalization"[2]. So we had revised the original sentence to "the FimH-positive *E. coli* can enter macrophages through caveolin-mediated endocytosis, which enables them to bypass lysosome processing and to maintain a stable nanostructure"[1, 2]. We hope these changes will meet the requirement. The updated description had been supplemented in the manuscript and marked in red in the revised manuscript.

Reference:

[1] Shin JS, Abraham SN. Co-option of endocytic functions of cellular caveolae by pathogens. Immunology. 2001, 102, 2-7.

[2] Baorto DM, Gao Z, Malaviya R, Dustin ML, van der Merwe A, Lublin DM, Abraham SN. Survival of FimH-expressing enterobacteria in macrophages relies on glycolipid traffic. Nature. 1997, 389, 636-639.

The revised parts were listed below:

The FimH-positive *E. coli* can enter macrophages through caveolin-mediated endocytosis, which enables them to bypass lysosome processing and to maintain a stable nanostructure[44, 45].

Response to Reviewer 2 Comments:

Thank you for addressing the reviewers' feedback. The addition of B16F10 data to Fig. 8 is informative. However, the figure should be reworked to coherently incorporate these additional data:

1. The schematic and caption for panel a should mention H22 or B16F10.

Response: Thank you for your kind comments. We had added panels a and i to Fig. 8 as "schematic of the orthotopic H22 tumour model experiment" and "schematic of the B16F10 tumour-bearing mouse model experiment", respectively. The corresponding captions had been improved. We hope these changes will meet the requirement. The revised description had been supplemented in the manuscript and marked in red in the revised manuscript.

The revised parts were listed below:

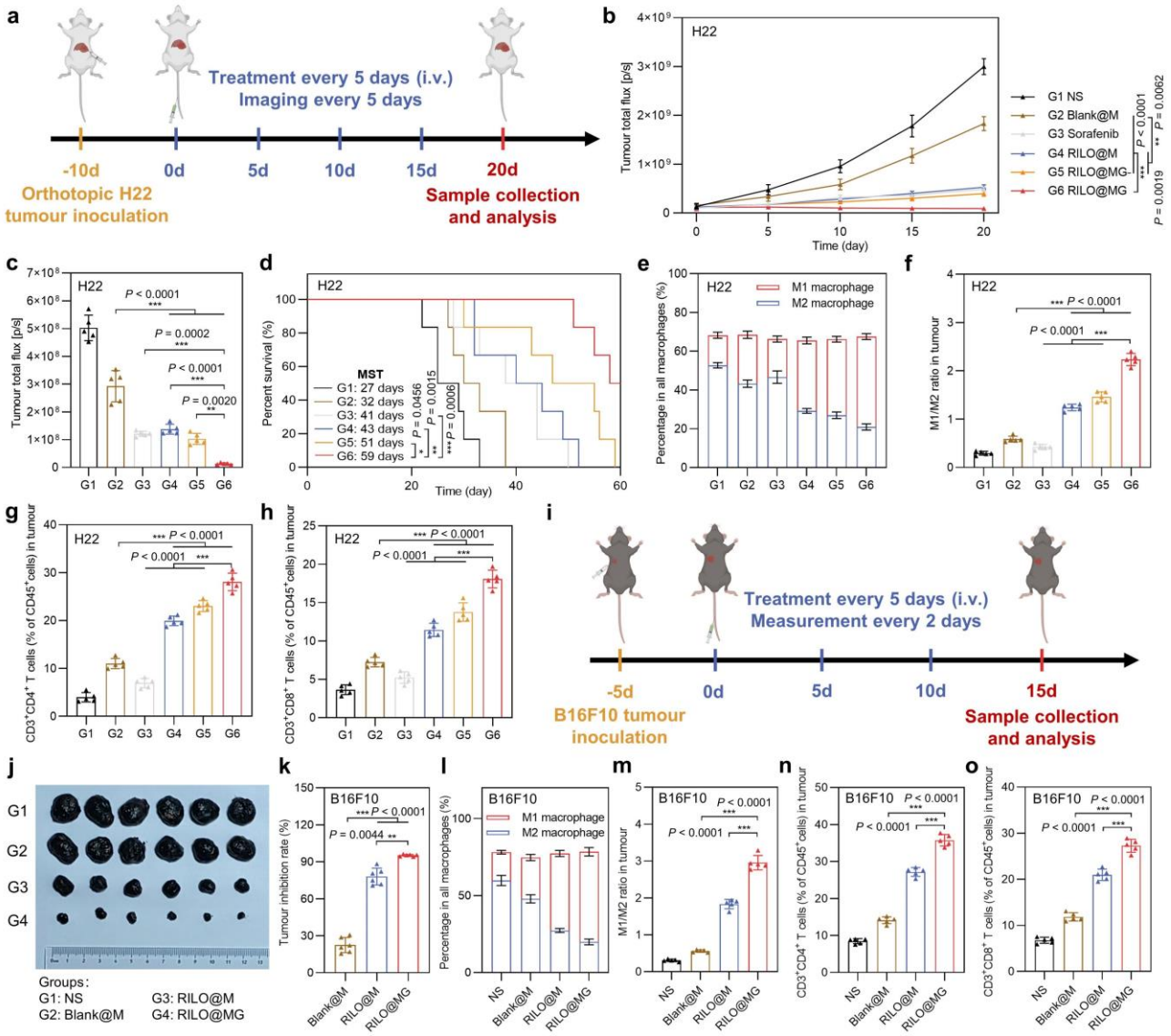

Fig. 8| Efficacy validation of RILO@MG in the orthotopic H22 tumour model and B16F10 tumour-bearing

mouse model. a, Schematic of the orthotopic H22 tumour model experiment (dose of 3.0 × 10^6 cells per mouse per injection, equal to 4 mg/kg R848 and 3.4 mg/kg INCB; sorafenib: 10 mg/kg). **b-d,** In vivo bioluminescence intensity curves (**b**), ex vivo livers on Day 20 of bioluminescence quantification (**c**) and animal survival (**d**) of the orthotopic H22 tumour model receiving the indicated treatments (n = 5 biologically independent animals for **b-c** and n = 6 biologically independent animals for survival). **e-h,** Flow cytometry quantitative data of M1-type macrophage and M2-type macrophage (**e, f**) and $CD4^+$ and $CD8^+$ T cells (**g, h**) in tumours of the orthotopic H22 tumour model sacrificed on Day 20 (n = 5 biologically independent animals). **i,** Schematic of the B16F10 tumour-bearing mouse model experiment (dose of 3.0 × 10^6 cells per mouse per injection, equal to 4 mg/kg R848 and 3.4 mg/kg INCB). **j, k,** Tumour photographs (**j**) and tumour inhibition rate (**k**) of the sacrificed B16F10 tumour-bearing mice at the study endpoint (n = 6 biologically independent animals). **l-o,** Flow cytometry quantitative data of M1-type macrophage and M2-type macrophage (**l, m**) and $CD4^+$ and $CD8^+$ T cells (**n, o**) in tumours of the sacrificed B16F10 tumour-bearing mice (n = 5 biologically independent animals). Data are expressed as the mean ± SD. One-way ANOVA with Tukey's multiple comparisons test (**c, f-h, m-o**), the Welch ANOVA with Dunnett's T3 multiple comparisons test (**k**), two-way ANOVA with repeated measures (**b**) and log-rank tests for survival data (**d**) were used for statistical analysis. $^{**}P < 0.01$; $^{***}P < 0.001$. BMDMs were used in all experiments involving macrophages.

2. Panels f-h should be labeled in the figure and the caption should refer to H22.

Response: Thank you for your kind comments. In the updated Fig. 8, panels f-h (equivalent to panels e-h in the revised manuscript) could be well distinguished. The corresponding captions had been improved. We hope these changes will meet the requirement.

3. Panels i-j should be labeled in the figure and the caption should refer to B16F10.

Response: Thank you for your kind comments. In the updated Fig. 8, panels i-j (equivalent to panels j-k in the revised manuscript) could be well distinguished. The corresponding captions had been improved. We hope these changes will meet the requirement.

4. Panels m and n need to be mentioned in the caption (and refer to B16F10).

Response: Thank you for your kind comments. In the updated Fig. 8, panels m-n (equivalent to panels l-o in the revised manuscript) could be well distinguished. The corresponding captions had been improved. We hope these changes will meet the requirement.

Response to Reviewer 3 Comments:

Accept

Response to Reviewer 4 Comments:

In Liu et. al, the authors describe a formulation and potential mechanism of action for an innovative cytotherapy strategy. They show through a directed design strategy that the cytotherapy alters the function of macrophages, protects mice from preclinical tumor models, and may lead to enhanced tumor specific T cell responses.

1. My major concern is the manuscript lacks organization and is overwhelmingly dense. This opinion was partially reflected in Reviewer 1's assessment. Although the authors did eliminate some primary figure panels, the supplement was expanded to 39 figures. A key recommendation was to simplify the study by focusing on necessary data.

One intent was reflection on study designs and necessary control groups in order to simplify description of RILO@MG effects. Simplification could greatly improve reader appreciation of their findings. For example, some experiments in figures 6 and 7 include 13 groups. This is concerning because the authors do not provide rationale or context to their study design, or justify why at times the groupwise differences are inconsistent. It is not adequate to state that the RILO@MG group is different from a group. Related, this may point to a statistical concern on multiple hypothesis testing.

Response: Thank you for your kind comments. Based on your concerns and in conjunction with the opinions you mentioned in Question 3, we had refined this manuscript.

First, we split this manuscript into two parts according to your requirements in the revised manuscript. Fig. 2-5 mainly described the results with "the preparation and functional characterization of RILO@MG", and Fig. 6-8 mainly describes the results with "the efficacy evaluation of preclinical animal models". According to your suggestion, we reduced some data in the revised manuscript, which could ensure the integrity of this manuscript and highlight the key findings. The corresponding labels have been modified and improved. We hope these changes will meet your requirement.

Second, we added design rationale of valuating efficacy in the preclinical models in the revised manuscript. In order to investigate the antitumour effects of different preparations in an H22

tumour-bearing mouse model, thirteen groups were necessary and the main principles were as follows. NS group was set as the blank control group. For a start, we set up R848, INCB, RI, RLO, ILO and RILO groups to prove the advantages of combining TLR7/8 agonists with IDO1 inhibitor (compared R848 and INCB groups with RI group), nanomedicine delivery (compared R848 and INCB groups with RLO and ILO groups) and co-loading drugs into one nanoparticle (compared RI group with RILO group). Next, we set up Blank@M, LO@MG, RILO, combination treatment of RILO and MG (RILO+MG) and RILO@MG groups to prove the necessary for "inner packing" strategy. Lastly, RILO@M and RILO@MG- groups were used to demonstrate the role of "surface anchoring" strategy and releasing drugs in exosome form, respectively. The experimental results were further described and discussed to greatly improve reader appreciation of our findings in the revised manuscript.

Third, according to your suggestion, we simplified some results by focusing on necessary data on the basis of the antitumour evaluation in H22 tumour-bearing mouse model. The analysis of immune cells infiltration in Fig. 7 was set to the following eight groups (NS, Blank@M, LO@MG, RILO, RILO@M, RILO@MG-, RILO+MG and RILO@MG), and the experimental results were further described and discussed. We hope these changes will meet the requirement. The revised description had been supplemented in the manuscript and marked in red in the revised manuscript.

The revised parts were listed below:

RILO@MG significantly improved antitumour efficacy in an H22 tumour-bearing mouse model.

We next evaluated the antitumour efficacy of RILO@MG in H22 tumour-bearing mice, which expressed GPC3. In order to investigate the antitumour effects of different preparations, the mice were randomly divided into thirteen groups for a single factor test and given four i.v. injections with one of the following formulations as in Fig. 6a. NS group was set as the blank control group. First, we set up R848, INCB, RI, RLO, ILO and RILO groups to prove the advantages of combining TLR7/TLR8 agonists with IDO1 inhibitor (compared R848 and INCB groups with RI group), nanomedicine delivery (compared R848 and INCB groups with RLO and ILO groups) and co-loading drugs into one nanoparticle (compared RI group with RILO group). Second, we set up Blank@M, LO@MG, RILO, combination treatment of RILO and MG (RILO+MG) and RILO@MG groups to prove the necessary for inner packing strategy. Third, RILO@M and RILO@MG- groups were used to demonstrate the role of surface anchoring strategy and releasing drugs in exosome form, respectively. Tumour volume was monitored after the first treatment. The RILO@MG group had the slowest trend of tumour growth, with almost no growth in tumour volume over 20 days (Fig. 6b,f). The combination of TLR7/TLR8 agonists and IDO1 inhibitors could simultaneously regulate the TAM phenotype and enhance T-cell viability to produce anti-tumour effects. The RILO group, with a 56.46±4.90% tumour inhibition rate, had a lower

tumour inhibition rate than that of the RLO ($P < 0.001$), ILO ($P < 0.001$) and RI group ($P < 0.05$), indicating the effectiveness of combination R848 and INCB, especially when co-loaded into the one particle (Supplementary Fig. 11). Compared with Blank@M and LO@MG groups, RILO@M, RILO@MG- or RILO@MG group resulted in smaller tumour volumes at the study endpoint ($P < 0.001$, $P < 0.001$, $P < 0.001$, Fig. 6b), indicating the necessity of modifying M1-type macrophagesfor drug delivery. Compared with RILO@MG, RILO+MG group exhibited only moderate antitumour effects, which proved that merely combination of RILO and MG did not trigger the antitumour effects, and more strongly indicated that only inner packing strategy could effectively inhibit tumour growth. Compared with RILO@MG, RILO@M only inhibited tumour growth by 73.72±3.24% under the same dose regimen ($P < 0.001$, Supplementary Fig. 11), which showed the antitumour role of GPC3-mediated targeting. The tumour volume in the RILO@MG group was 102.49±16.78 mm^3, which was significantly smaller than that in the RILO@MG- group ($P < 0.001$, Fig. 6b), suggesting that the release form of RI-exosomes contributed to the promotion of antitumour efficacy. These data fully demonstrated the contribution of the surface anchoring and inner packing strategies to antitumour efficacy.

Mice in each group were euthanized and dissected at 20 days post-first treatment, and the major organs and tumours were collected for analysis. Consistent with the tumour growth profiles of the analysed tumours, the tumours in the RILO@MG group were the smallest in all the groups, as shown in the tumour weights and tumour images (Fig. 6c, d). Based on the results of Ki-67 immunohistochemistry, haematoxylin and eosin (H&E) staining and TUNEL immunofluorescence, we analysed the proliferation and apoptosis of tumours. The sectioning results showed that the RILO@MG group had more tumour cell apoptosis and less tumour cell proliferation (Supplementary Fig. 12). In addition, none of the groups showed significant loss of body weight at the study endpoint (Fig. 6e) or tissue damage (Supplementary Fig. 13). Furthermore, RILO@MG did not cause the appearance of a cytokine storm after initial administration, which would be evident by elevated serum IL-6 and TNF-α levels, a significant change in the organ/body weight ratio at the study endpoint and an increase in the levels of liver or kidney injury markers at the study endpoint (BUN, LDH, ALT, AST and ALP, Supplementary Fig. 14). These results confirmed that RILO@MG had preliminary safety and efficacy in H22 tumour-bearing mice.

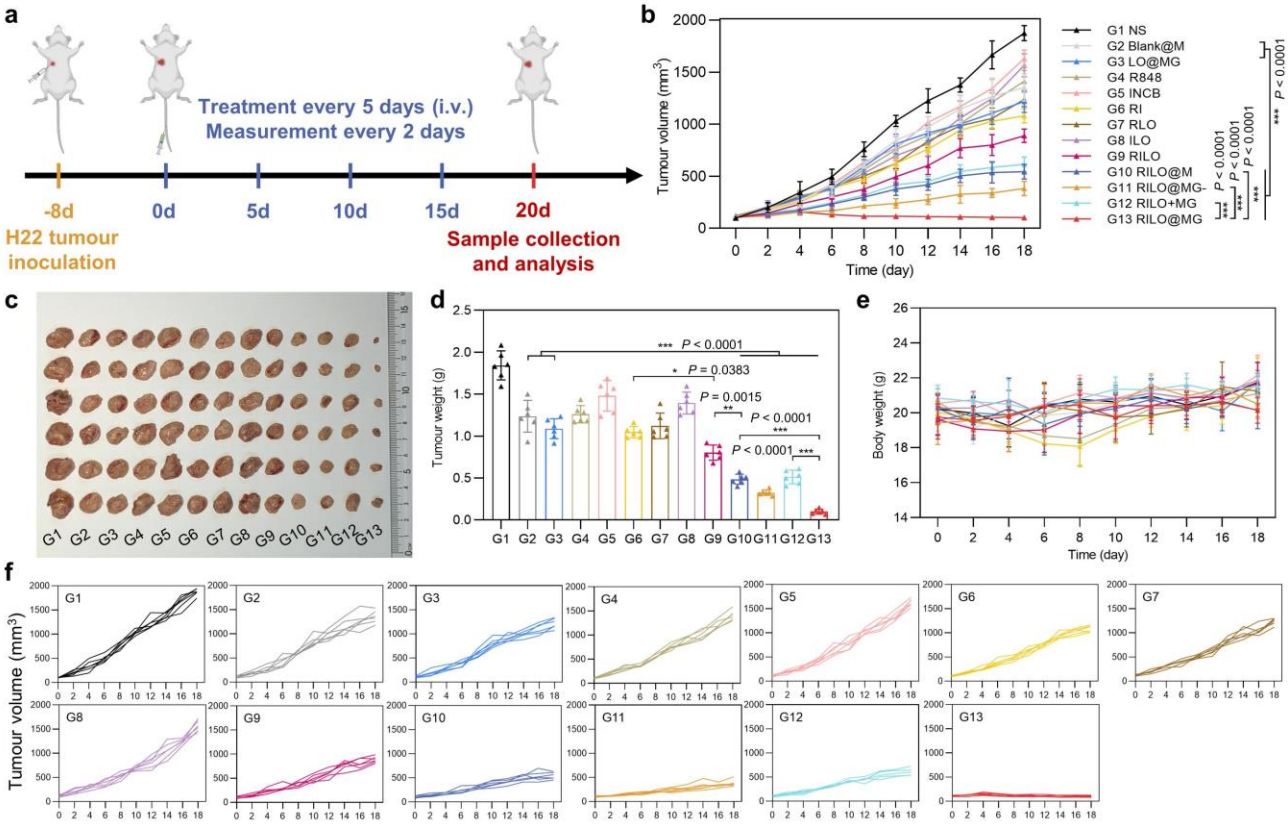

Fig. 6| The antitumour activity of RILO@MG in an H22 tumour-bearing mouse model. a, Regimen of i.v. administration in H22 tumour-bearing mice (at a dosage of 3.0×10^6 cells per mouse per injection, equal to 4 mg/kg R848 and 3.4 mg/kg INCB). Mice requiring injected formulations made by M1-type macrophages each received the equivalent number of cells (3.0×10^6 cells per mouse). Mice requiring injection of other formulations each received the equivalent dose of medicine (4 mg/kg R848 and 3.4 mg/kg INCB). When the tumour volumes reached ~2,000 mm^3, the mice were sacrificed. **b-f,** Average tumour growth curves (**b**), tumour photographs (**c**), tumour weights (**d**), body weight changes (**e**) and individual tumour growth curves (**f**) of H22 tumour-bearing mice receiving the indicated treatments ($n = 6$ biologically independent animals per group). Data are expressed as the mean ± SD. One-way ANOVA with Tukey's multiple comparisons test (**d**) or two-way ANOVA with repeated measures (**b**) was used for statistical analysis. *$P < 0.05$; **$P < 0.005$; ***$P < 0.001$. BMDMs were used in all experiments involving macrophages.

RILO@MG reversed the suppressive TME by regulating the TAM phenotype and enhancing T-cell viability, and produced long-term immune memory in an H22 tumour-bearing mouse model.

The frequencies of immune cells (M1-type macrophage, M2-type macrophage, $CD69^+$ T cell, $CD4^+$ T cell, $CD8^+$ T cell, CTL and Treg) and the concentrations of cytokines (including IFN-γ, IL-12p70, TNF-α, IL-10, TGF-β1 and IL-4) in tumour tissues collected on Day 20 and the frequencies of effector memory T-cell in spleens collected on Day 20 were used to monitor the changes in immune status of the TME (Fig. 7a).

To evaluate the overall immune status of the tumour, we first measured the levels of intratumoural cytokines. The heatmap showed that mice given RILO@MG had increased intratumoural levels of immunostimulatory cytokines, including IFN-γ, IL-12p70 and TNF-α, along with reduced intratumoural levels of immunosuppressed cytokines, including IL-10, TGF-β1 and IL-4 (Fig. 7b), indicating that RILO@MG had an immunomodulatory effect. Encouraged by these expected results, we next examined the tumour infiltration of immune cells.

Recent preclinical and clinical insights indicated that macrophages were the most abundant nonneoplastic critical effector cells of cancer immunotherapy in the TME[51, 52]. The population of M1-type macrophages within the TME of mice in the RILO@MG group was 3.19-fold higher than that in the NS group, and the opposite trend was observed for M2-type macrophages (Fig. 7c and Supplementary Fig. 16a, b). The M1/M2 ratio in the RILO@M group was higher than that in the RILO group ($P < 0.001$, Fig. 7d), implying that inner RILO packing of M1-type macrophages could repolarize M2-type macrophages to M1-type macrophages in vivo. Compared with the Blank@M, LO@MG and RILO@MG- groups, RILO@MG had the highest M1/M2 ratio ($P < 0.001$, $P < 0.001$, $P < 0.001$), which implied that the released drugs, especially in exosome form, played a key role in M2-to-M1 reversion of macrophage in tumour. This conclusion was in agreement with the experimental results verified in vitro (Fig. 5g).

Based on the fact that T cells played a key role in the immunotherapy achieved by RILO@MG (Fig. 5k, l), we further evaluated the frequencies of multiple intratumoural T cell subtypes. CD69 was one of the earliest markers of upregulation after T-cell activation,and CTL-infiltrating tumour tissues are generally considered the primary mediator of tumour killing. The RILO@MG and RILO@M groups revealed a higher percentage than the RILO group about $CD69^+$ T cells ($P < 0.001$, $P < 0.001$, Fig. 7e and Supplementary Fig. 16c), $CD4^+$ T cells ($P < 0.001$, $P < 0.001$, Fig. 7f and Supplementary Fig. 16d), $CD8^+$ T cells ($P < 0.001$, $P < 0.01$, Fig. 7g) and CTLs (IFN-γ^+CD8^+ T cells) ($P < 0.001$, $P < 0.001$, Fig. 7i and Supplementary Fig. 16f), indicating that packing RILOs in M1-type macrophages was required to further enhance the activation of multiple T cells in tumour tissue. Next, the RILO@MG group greatly decreased the proportion of Tregs compared with the other groups (Fig. 7h and Supplementary Fig. 16e). Considering the antitumour role of GPC3-mediated targeting, we focused on comparing the immune cell changes between RILO@M group and RILO@MG group. Significantly, the RILO@MG group had more $CD69^+$ T cells, $CD4^+$ T cells, $CD8^+$ T cells and CTLs (IFN-γ^+CD8^+ T cells), and fewer Tregs than the RILO@M group, showing better immune cell regulation in tumour tissues (Fig. 7e-i). These results collectively suggested that RILO@MG could change the immune status of the TME from immune suppressive to immune active, thus promoting the antitumour immune response.

Additionally, RILO@MG treatment resulted in the highest percentage of effector memory ($CD44^+CD62L^-$) $CD8^+$ T cells compared with that after treatment with the other macrophage-based formulations (Fig. 7j and Supplementary Fig. 17a). We were thus interested in determining whether RILO@MG could induce memory immune responses. To establish a rechallenged tumour model, H22 tumour-bearing mice that had been treated four times were reinoculated with H22 cells (Fig. 7k). Rechallenged tumours in mice administered RILO@MG were significantly delayed, while rapid growth was observed in the NS group (Fig. 7m and Supplementary Fig. 17b). Remarkably, two out of five mice were still tumour free on Day 36 in the RILO@MG group (Fig. 7l). These data indicated that RILO@MG could effectively activate the long-term antitumour response and effectively inhibit tumour growth in mice.

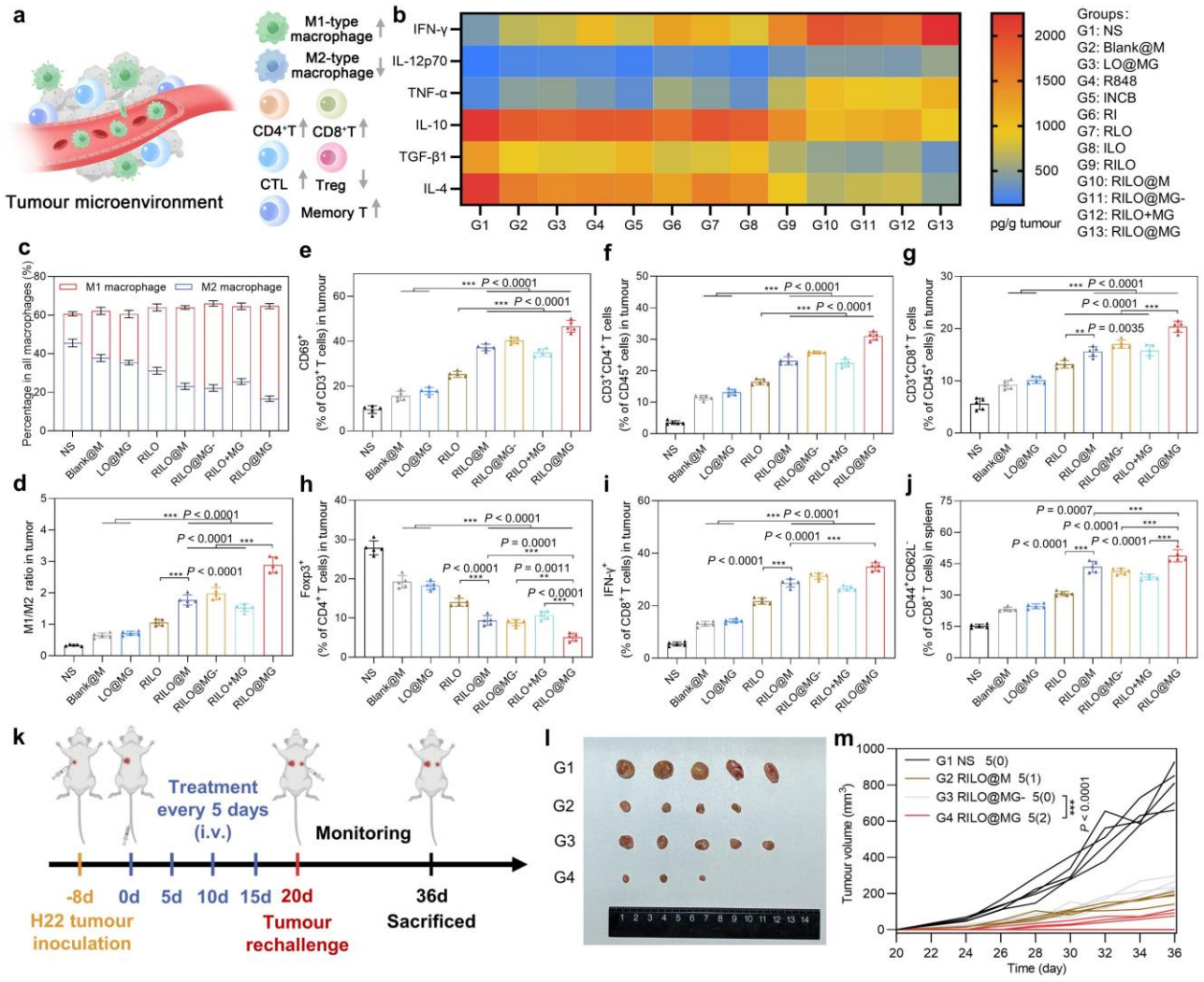

Fig. 7| The RILO@MG regulates TAM phenotype and enhances T-cell viability to remodel the suppressive TME in an H22 tumour-bearing mouse model. a, Schematic diagram of the regulatory effect of RILO@MG on the immunosuppressive TME, indicating an increase about immune-active cells and a decrease in the proportion of immune-suppressing cells within the TME. **b,** H22 tumour-bearing mice were treated as in Fig. 6a. The intratumoural levels of cytokines were quantified using ELISA analysis at the study endpoint. **c-i,** H22 tumour-bearing mice were treated as in Fig. 6a. Flow cytometric analysis of M1-type macrophage and M2-type macrophage (**c, d**), $CD69^+$ T cells (**e**), $CD4^+$ T cells (**f**), $CD8^+$ T cells (**g**), $CD4^+Foxp3^+$ T cells (**h**), and $CD8^+IFN\text{-}\gamma^+$ T cells (**i**) within the TME. **j,** Flow cytometric analysis quantification of effector memory ($CD44^+CD62L^-$) $CD8^+$ T cells in spleens. **k,** Experimental timeline of rechallenged tumour model establishment. **l,** Secondary tumour photographs of the sacrificed mice at the study endpoint. **m,** Rechallenged tumour growth curves of tumour-bearing mice were monitored over time. The dosage regimen of all data in Fig. 7 was the same as that shown in Fig. 6a. Data are expressed as the mean ± SD with 5 biologically independent animals per group and was processed by one-way ANOVA with Tukey's multiple comparisons test (**c-j**) or two-way ANOVA with repeated measures (**m**). $^{**}P < 0.01$; $^{***}P < 0.001$. BMDMs were used in all experiments involving macrophages.

2. Although the authors provide Bonferroni post-hoc p-values for One-Way ANOVA assessments, they never indicate if the overall ANOVA p-values meet significance criteria to pursue post-hoc tests. Indeed, rebuttal statements to reviewer 2 may reflect some basic misunderstanding on

ANOVA and attributes of chosen post-hoc tests. In this regard, several experiments misuse ANOVA based on the statistical assumptions or normal distribution and independent samples (eg. 8k, 7b, 7i).

Response: Thank you for your kind comments. We are very sorry for the misunderstanding caused by the unclear description. We agree with you and think that the normality test and the homogeneity test of variance were the default prerequisites for statistical analysis, we did not describe them in detail in the previous manuscript. We apologized for the misunderstanding caused to you.

In the revised manuscript, we have supplemented the normality test and the homogeneity test of variance, specifically as follows: The data are expressed as the mean ± SD and the Shapiro-Wilk normality test was performed for evaluation of normal distribution. The data meet the homogeneity test of variance, the one-way ANOVA with Tukey's multiple comparisons test among multiple groups or two-tailed Student's t test among two groups was used for statistical significance calculation. The data do not meet the homogeneity test of variance, the Welch ANOVA with Dunnett's T3 multiple comparisons test among multiple groups or two-tailed Student's t test with Welch's correction among two groups was used for statistical significance calculation. The two-way ANOVA with Tukey's multiple comparisons test was used when two non-repeated measure parameters were considered. Further, the two-way ANOVA with repeated measures was used to analyze the effect of different formulations on tumour growth over time, the Geisser-Greenhouse correction was used when Mauchly's test of sphericity was not satisfied, and Tukey's post hoc test was used for inter-group comparison.

Further, we revised the statistical significance using two-way ANOVA, including figures 3b-c, 5d, S5 and S6a-b. We revised the statistical significance using two-way ANOVA with repeated measures, including figures 6b, 7m, 8b, S10b and S17c (equivalent to figure 7m in the revised manuscript). For two-way ANOVA with repeated measures, the main effect of group factor, the main effect of time factor, and the interaction between group and time had statistically significant on tumour volume ($P < 0.001$). The numerical data were matched between the figures and the source data.

To sum up, according to your suggestion, we had described the statistical analysis in detail in the revised manuscript. We hope these changes will meet the requirement. The revised description and figures had been supplemented in the manuscript and marked in red in the revised manuscript.

The revised parts were listed below:

24 Statistical analysis and schematic illustrations. GraphPad Prism 8 was used for statistical analyses. The data are expressed as the mean ± SD and the Shapiro-Wilk normality test was performed for evaluation of normal distribution. The data meet the homogeneity test of variance, the one-way ANOVA with Tukey's multiple comparisons test among multiple groups or two-tailed Student's t test among two groups was used for statistical significance calculation. The data do not meet the homogeneity test of variance, the Welch ANOVA with Dunnett's T3 multiple comparisons test among multiple groups or two-tailed Student's t test with Welch's correction among two groups was used for statistical significance calculation. The two-way ANOVA with Tukey's multiple comparisons test was used when two non-repeated measure parameters were considered. Further, the two-way ANOVA with repeated measures was used to analyze the effect of different formulations on tumour growth over time, the Geisser-Greenhouse correction was used when Mauchly's test of sphericity was not satisfied, and Tukey's post hoc test was used for inter-group comparison. $*P < 0.05$, $**P < 0.01$ and $***P < 0.001$ were considered statistically significant. Schematic illustrations of Fig. 1, 2a, 5a, 5i and 7a were created by ourselves with Adobe Illustrator. Schematic illustrations of Fig. 3a, 5g, 5k, 6a, 7k, 8a, 8i and Supplementary Fig. 3a were created by ourselves with Microsoft PowerPoint 2021 using icons from Biorender.com (Agreement number: CN25R9Z54P).

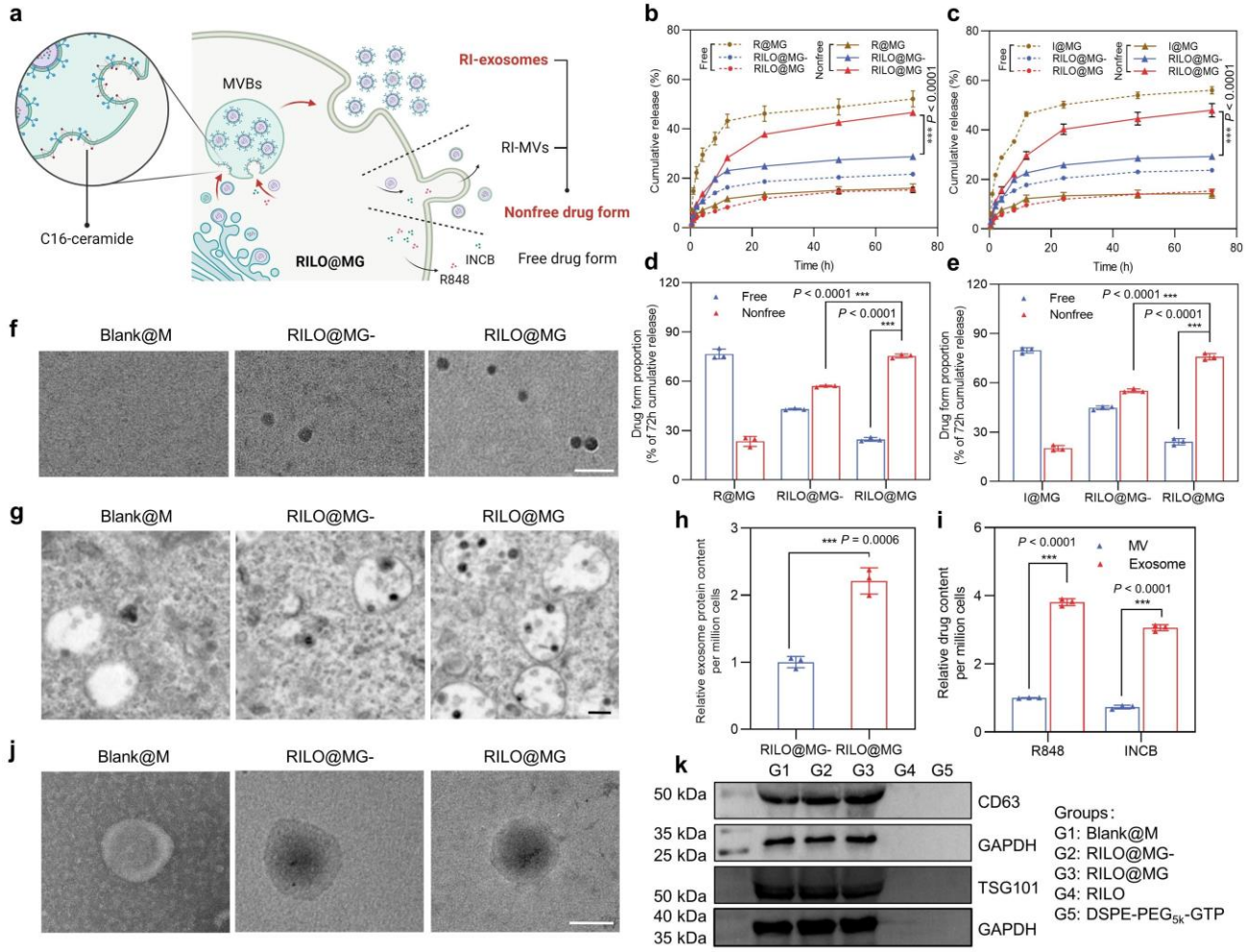

Fig. 3| RILOs are released from RILO@MG in the form of RI-exosomes. a, Schematic illustration of regulating the release form of the RILOs packed in RILO@MG. **b-e,** Release profiles during 72 h for R848 (**b**) or INCB (**c**) and the proportion of cumulative release at 72 h for R848 (**d**) or INCB (**e**) of free drug form or nonfree drug form from different groups, respectively (n = 3 biologically independent experiments). **f,** Representative TEM analyses about released media from Blank@M, RILO@MG- and RILO@MG groups at 24 h after preparation (n = 3 biologically independent experiments). Scale bar, 200 nm. **g,** Representative TEM images showed increasing MVBs and ILVs formation containing RILO in RILO@MG with the help of C16-ceramide (n

= 3 biologically independent experiments). Scale bar, 200 nm. **h,** The relative released exosome protein content 24 h after RILO@MG- and RILO@MG were prepared (*n* = 3 biologically independent experiments). **i,** R848 and INCB content encapsulated in exosomes or MVs by RILO@MG as measured by HPLC, indicating that the drugs were mostly contained in exosomes, not MVs (*n* = 3 biologically independent experiments). **j,** TEM images of exosomes from Blank@M and RI-exosomes from RILO@MG- and RILO@MG (*n* = 3 biologically independent experiments). Scale bar, 50 nm. **k,** Detection of exosome markers (CD63 and TSG101) of released exosomes from different groups by western blotting (*n* = 3 biologically independent experiments). Data are expressed as the mean ± SD. Two-tailed Student's *t* test (**d, e, h, i**) or two-way ANOVA with Tukey's multiple comparisons test (**b, c**) was carried out for statistical analysis. **P* < 0.05; ****P* < 0.001. BMDMs were used in all experiments involving macrophages.

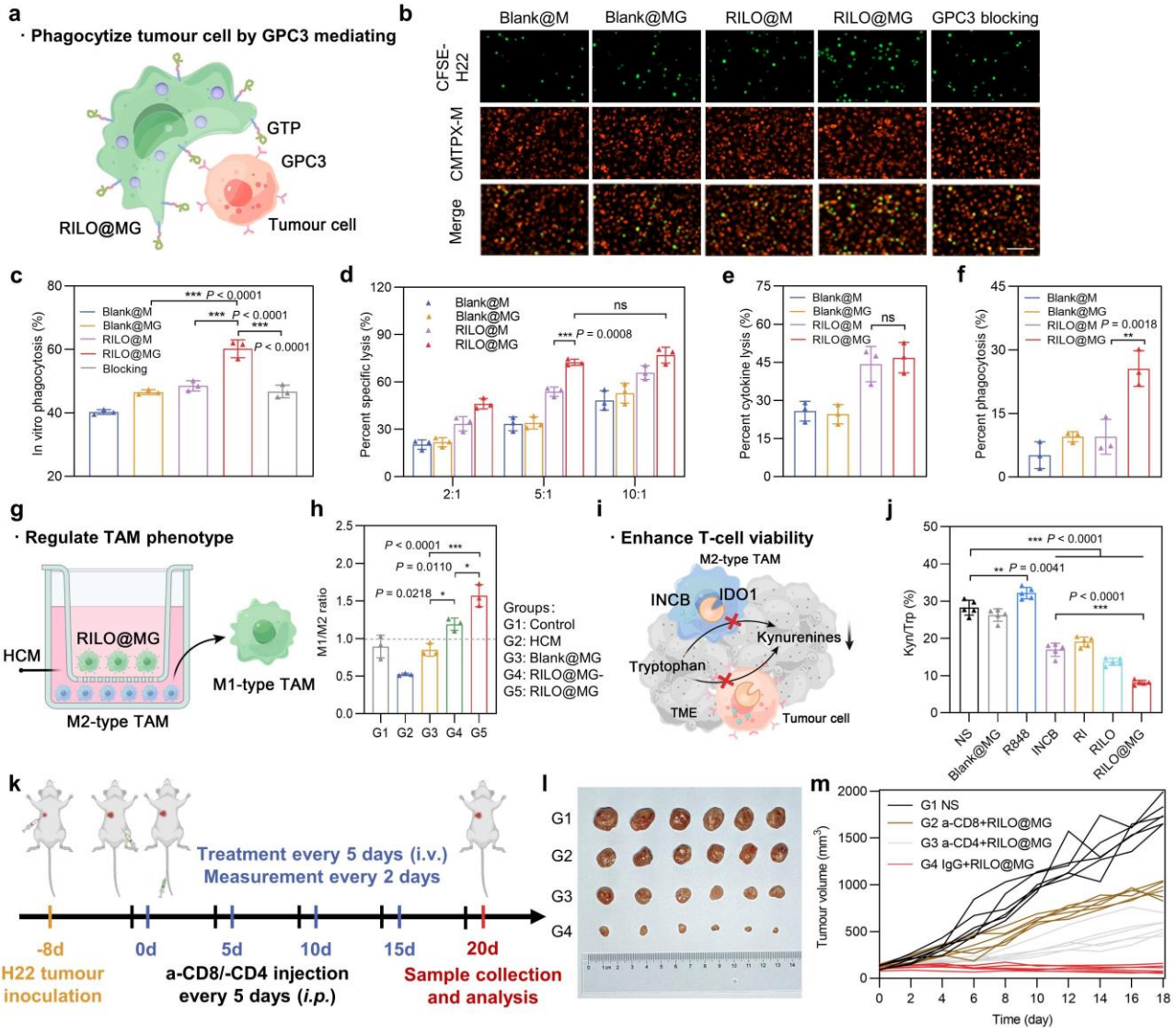

Fig. 5| RILO@MG promotes antitumour immunity by specifically phagocytizing tumour cells, regulating the TAM phenotype and enhancing T-cell viability. a, Schematic illustration of RILO@MG phagocytizing H22 cells mediated by GPC3 and GTP. **b,** Fluorescence microscopy images of different formulations after coculture with H22 cells for 4 hours (E:T = 2:1). Scale bar = 100 μm. E:T, effector cell (different formulations prepared using M1-type macrophage) to target cell (H22 cell) ratio. **c,** Anchoring of GTP on RILO@MG promoted the

phagocytosis of H22 cells (n = 3 biologically independent experiments). Different formulations were cocultured with H22 cells for 4 h (E:T = 1:1) and evaluated by flow cytometric analysis. **d,** Specific lysis of H22 cells after coculture for 12 h at different E:T ratios measured by CCK-8 assay (n = 3 biologically independent experiments). **e, f,** Percent cytokine lysis (**e**) and phagocytosis lysis (**f**) of H22 cells after coculture with different formulations for 12 h (E:T = 5:1) by using Transwell plates (pore size 0.4 μm) (n = 3 biologically independent experiments). **g,** Experimental process for promoting the polarization from M2 phenotype to M1 phenotype. **h,** Phenotype analysis of TAMs after coculture with different formulations in HCM for 24 h (n = 3 biologically independent experiments). **i,** Schematic illustration of RILO@MG enhancing T cells by inhibiting the production of Kyn. **j,** IDO1 activity was evaluated according to the percentage of Kyn/Trp within tumours (n = 5 biologically independent animals per group). **k,** Regimen of the antitumour experiment after removal of $CD4^+$ or $CD8^+$ T cells. **l, m,** Photographs of tumours (**l**) and individual tumour growth curves (**m**) showed the critical role of T cells in antitumour immunity mediated by RILO@MG (n = 6 biologically independent animals per group). Data are expressed as the mean ± SD and were processed by one-way ANOVA with Tukey's multiple comparisons test (**c, e-f, h, j**) or two-way ANOVA with Tukey's multiple comparisons test (**d**). *P < 0.05; **P < 0.01; ***P < 0.001; ns, no significance. BMDMs were used in all experiments involving macrophages.

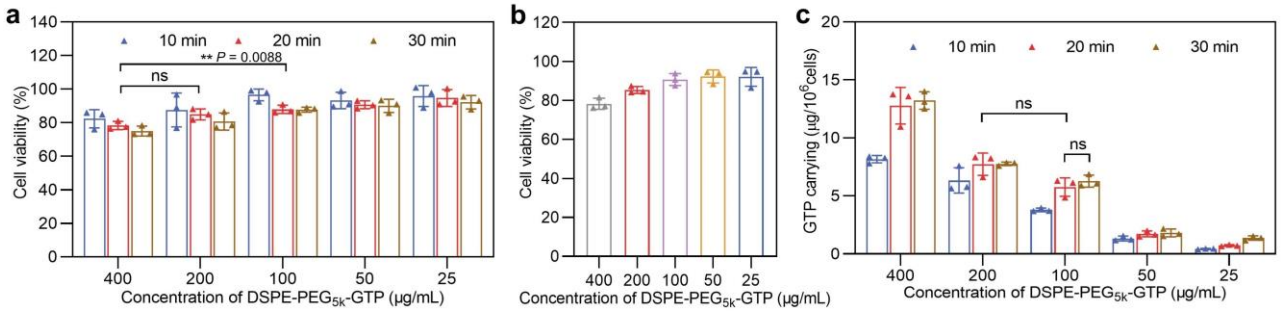

Supplementary Fig. 5. The optimizations of incubation concentrations and time on cell viability and GTP carrying. a, In vitro cell viability of different incubation concentrations and time of DSPE-PEG_{5k}-GTP on $RILO@M^{RAW}$. **b,** In vitro cell viability of different incubation concentrations of DSPE-PEG_{5k}-GTP on $RILO@M^{BMDM}$ for incubating 20 min. **c,** The GTP carrying of different incubation concentrations and time of DSPE-PEG_{5k}-GTP on $RILO@M^{RAW}$. In addition, the GTP carrying of $RILO@MG^{BMDM}$ was 6.67±0.64 μg/10^6cells at the optimal incubation concentration and time, which slightly higher than $RILO@MG^{RAW}$ (5.76±0.79 μg/10^6cells). However, there was no significant difference between them, which were analysed by the two-tailed Student's t-test. Data are expressed as the mean ± SD with 3 biologically independent experiments. Two-way ANOVA with Tukey's multiple comparisons test (**a, c**) was carried out for statistical analysis. **P < 0.01; ns, no significance.

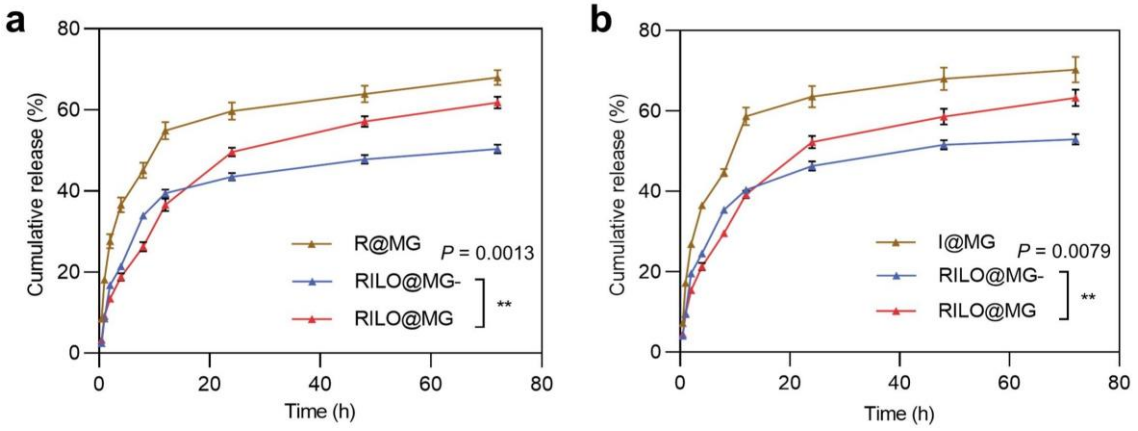

Supplementary Fig. 6. Release profiles of total drugs from RILO@MG. a, Release profiles during 72 h of total R848 from RILO@MG (n = 3 biologically independent experiments). **b,** Release profiles during 72 h of total INCB from RILO@MG (n = 3 biologically independent experiments). All data are shown as the mean ± SD and the data were analysed by two-way ANOVA with Tukey's multiple comparisons test. $^{**}P < 0.01$.

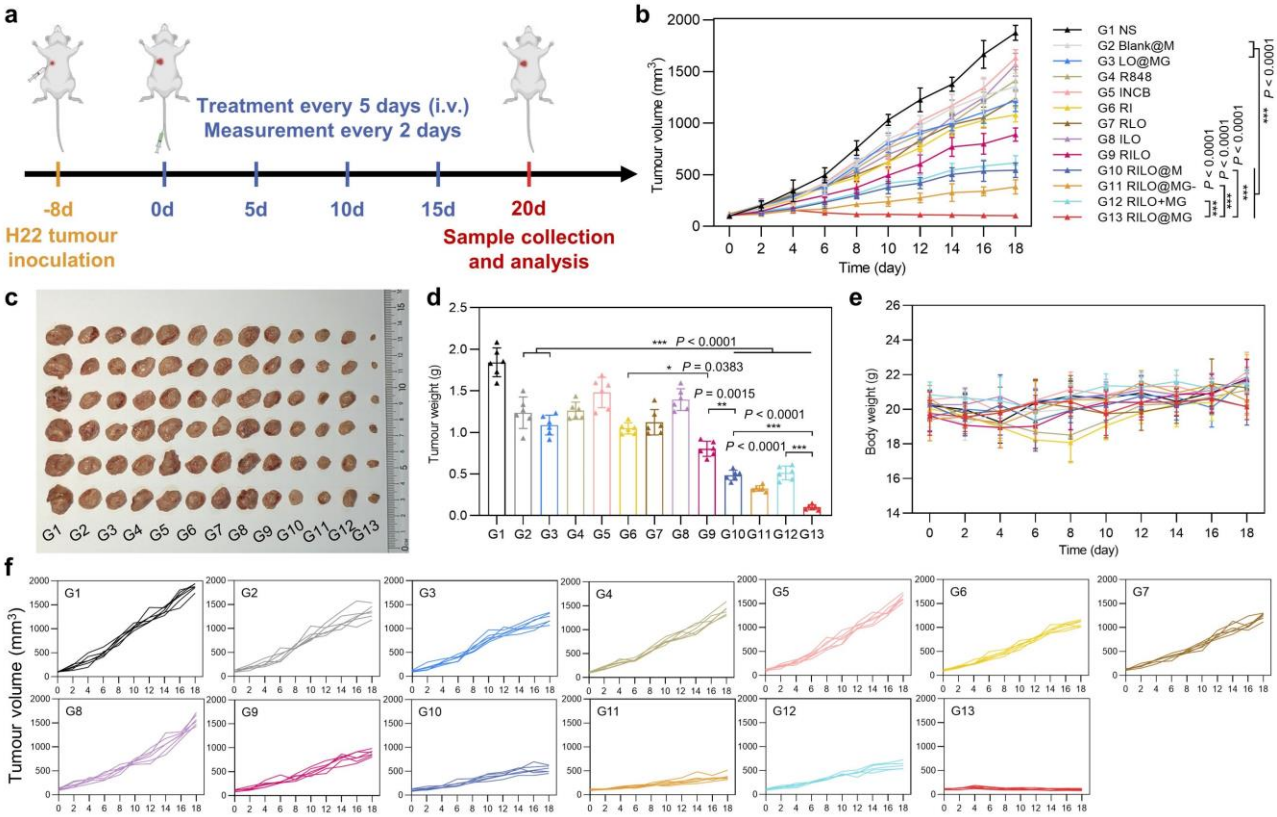

Fig. 6| The antitumour activity of RILO@MG in an H22 tumour-bearing mouse model. a, Regimen of i.v. administration in H22 tumour-bearing mice (at a dosage of 3.0 × 10^6 cells per mouse per injection, equal to 4 mg/kg R848 and 3.4 mg/kg INCB). Mice requiring injected formulations made by M1-type macrophages each received the equivalent number of cells (3.0 × 10^6 cells per mouse). Mice requiring injection of other formulations each received the equivalent dose of medicine (4 mg/kg R848 and 3.4 mg/kg INCB). When the tumour volumes reached ~2,000 mm^3, the mice were sacrificed. **b-f,** Average tumour growth curves (**b**), tumour photographs (**c**), tumour weights (**d**), body weight changes (**e**) and individual tumour growth curves (**f**) of H22 tumour-bearing mice receiving the indicated treatments (n = 6 biologically independent animals per group). Data are expressed as the mean ± SD. One-way ANOVA with Tukey's multiple comparisons test (**d**) or two-way ANOVA with repeated

measures (**b**) was used for statistical analysis. *$P < 0.05$; **$P < 0.005$; ***$P < 0.001$. BMDMs were used in all experiments involving macrophages.

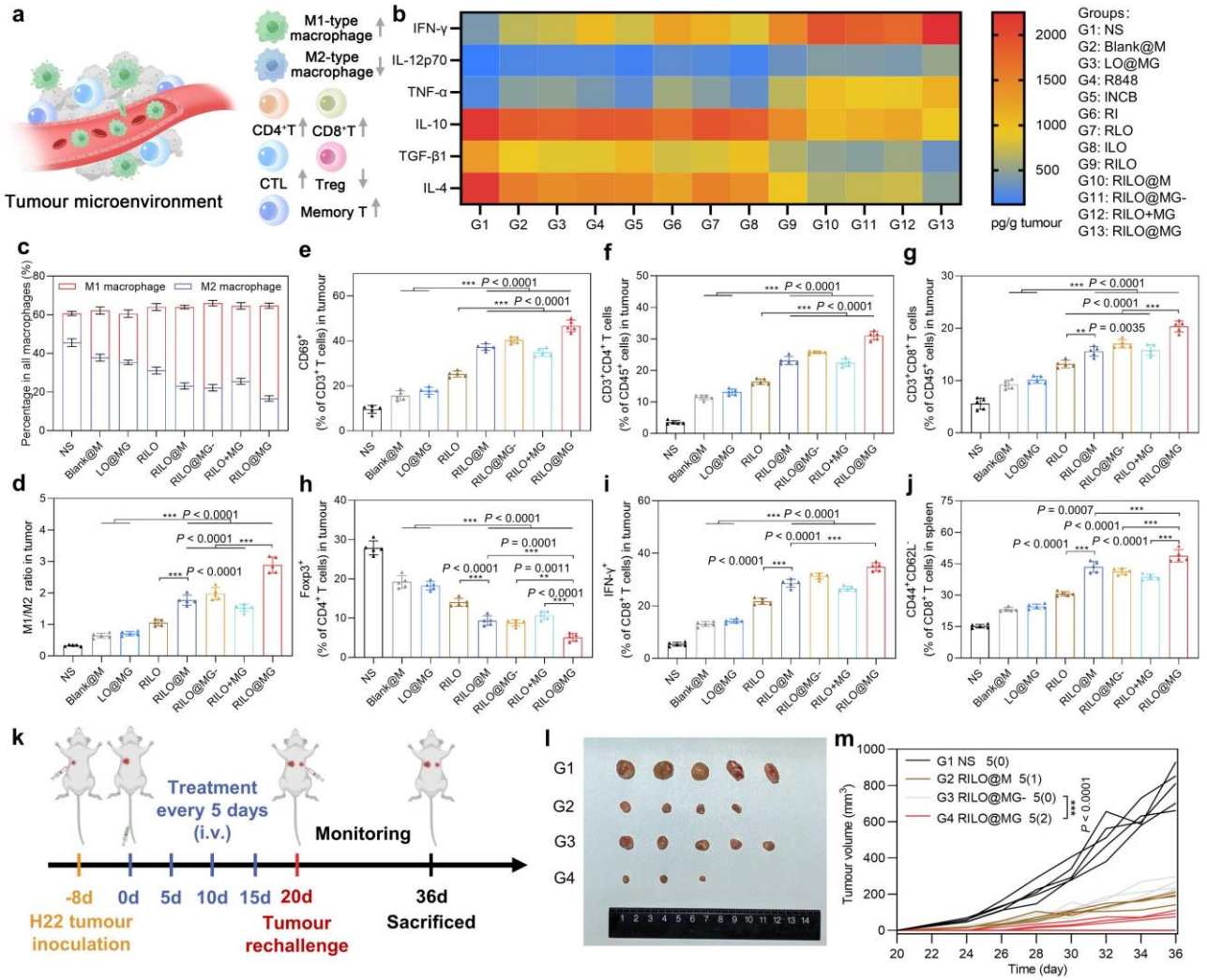

Fig. 7| The RILO@MG regulates TAM phenotype and enhances T-cell viability to remodel the suppressive TME in an H22 tumour-bearing mouse model. a, Schematic diagram of the regulatory effect of RILO@MG on the immunosuppressive TME, indicating an increase about immune-active cells and a decrease in the proportion of immune-suppressing cells within the TME. **b,** H22 tumour-bearing mice were treated as in Fig. 6a. The intratumoural levels of cytokines were quantified using ELISA analysis at the study endpoint. **c-i,** H22 tumour-bearing mice were treated as in Fig. 6a. Flow cytometric analysis of M1-type macrophage and M2-type macrophage (**c, d**), $CD69^+$ T cells (**e**), $CD4^+$ T cells (**f**), $CD8^+$ T cells (**g**), $CD4^+Foxp3^+$ T cells (**h**), and $CD8^+IFN\text{-}\gamma^+$ T cells (**i**) within the TME. **j,** Flow cytometric analysis quantification of effector memory ($CD44^+CD62L^-$) $CD8^+$ T cells in spleens. **k,** Experimental timeline of rechallenged tumour model establishment. **l,** Secondary tumour photographs of the sacrificed mice at the study endpoint. **m,** Rechallenged tumour growth curves of tumour-bearing mice were monitored over time. The dosage regimen of all data in Fig. 7 was the same as that shown in Fig. 6a. Data are expressed as the mean ± SD with 5 biologically independent animals per group and was processed by one-way ANOVA with Tukey's multiple comparisons test (**c-j**) or two-way ANOVA with repeated measures (**m**). **$P < 0.01$; ***$P < 0.001$. BMDMs were used in all experiments involving macrophages.

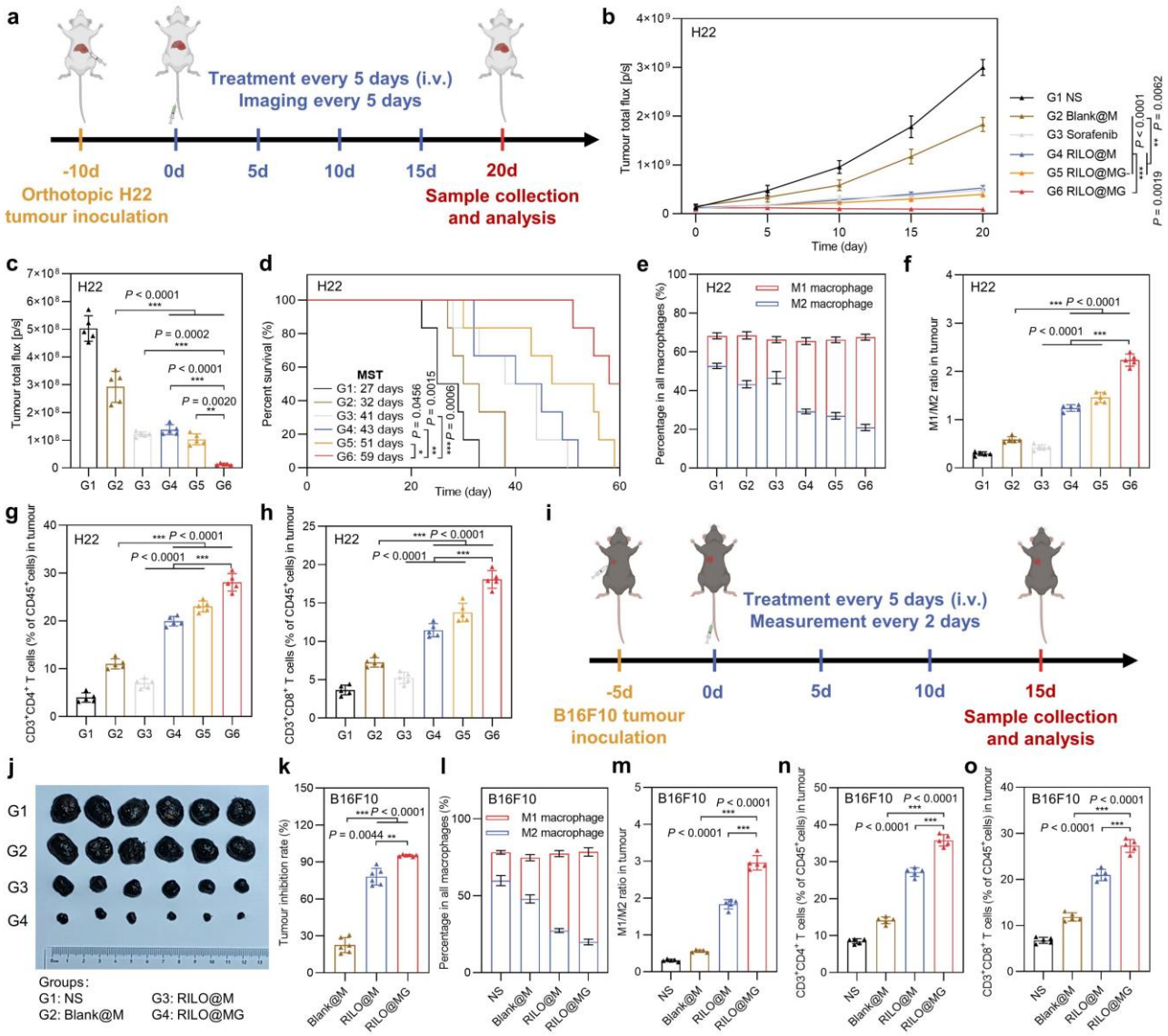

Fig. 8| Efficacy validation of RILO@MG in the orthotopic H22 tumour model and B16F10 tumour-bearing mouse model. a, Schematic of the orthotopic H22 tumour model experiment (dose of 3.0 × 10^6 cells per mouse per injection, equal to 4 mg/kg R848 and 3.4 mg/kg INCB; sorafenib: 10 mg/kg). **b-d,** In vivo bioluminescence intensity curves (**b**), ex vivo livers on Day 20 of bioluminescence quantification (**c**) and animal survival (**d**) of the orthotopic H22 tumour model receiving the indicated treatments (n = 5 biologically independent animals for **b-c** and n = 6 biologically independent animals for survival). **e-h,** Flow cytometry quantitative data of M1-type macrophage and M2-type macrophage (**e, f**) and $CD4^+$ and $CD8^+$ T cells (**g, h**) in tumours of the orthotopic H22 tumour model sacrificed on Day 20 (n = 5 biologically independent animals). **i,** Schematic of the B16F10 tumour-bearing mouse model experiment (dose of 3.0 × 10^6 cells per mouse per injection, equal to 4 mg/kg R848 and 3.4 mg/kg INCB). **j, k,** Tumour photographs (**j**) and tumour inhibition rate (**k**) of the sacrificed B16F10 tumour-bearing mice at the study endpoint (n = 6 biologically independent animals). **l-o,** Flow cytometry quantitative data of M1-type macrophage and M2-type macrophage (**l, m**) and $CD4^+$ and $CD8^+$ T cells (**n, o**) in tumours of the sacrificed B16F10 tumour-bearing mice (n = 5 biologically independent animals). Data are expressed as the mean ± SD. One-way ANOVA with Tukey's multiple comparisons test (**c, f-h, m-o**), the Welch ANOVA with Dunnett's T3 multiple comparisons test (**k**), two-way ANOVA with repeated measures (**b**) and

log-rank tests for survival data (**d**) were used for statistical analysis. $^{**}P < 0.01$; $^{***}P < 0.001$. BMDMs were used in all experiments involving macrophages.

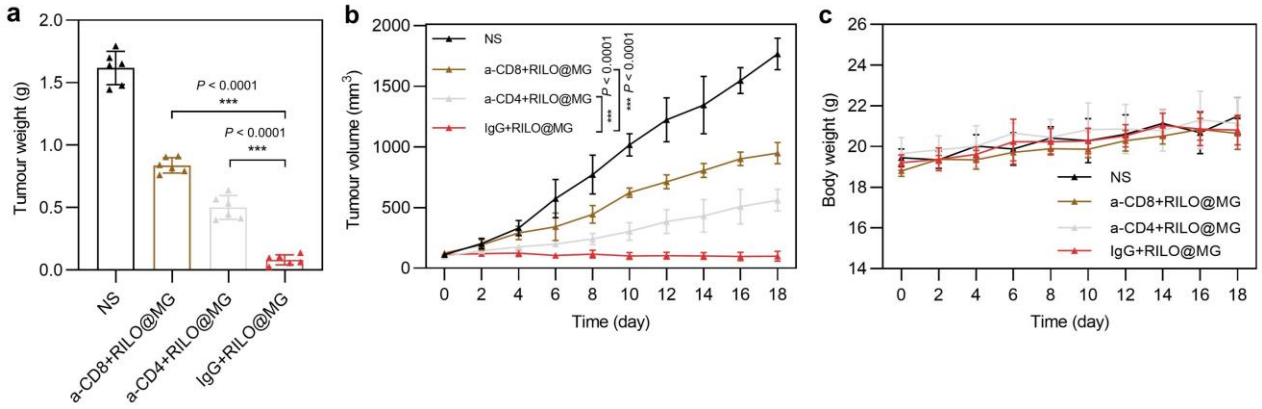

Supplementary Fig. 10. Tumour weights, average tumour growth curves and body weight changes over the course of treatment related to Fig. 5k-m. a, Tumour weights of H22 tumour-bearing mice (n = 6 biologically independent animals per group). **b**, Average tumour growth curves of H22 tumour-bearing mice (n = 6 biologically independent animals per group). **c,** body weight changes of H22 tumour-bearing mice (n = 6 biologically independent animals per group). All data are shown as the mean ± SD. One-way ANOVA with Tukey's multiple comparisons test (**a**) and two-way ANOVA with repeated measures (**b**) were carried out for statistical analysis. $^{***}P < 0.001$.

3. My opinion stands that the relative impact of this study may be improved by splitting it into two parts: one part describing results with "formulating the macrophage drug deliver(sic) system"; the second part evaluating the "efficacy in the preclinical models." Sections valuating efficacy in the preclinical models are lacking in design, development, and rationale. Although evidence is generally supportive, the relevant aspects in the results and discussion are not well developed. This concern may be true for the drug design aspects as well.

Although the premise remains interesting and of potentially high biomedical significance, there are critical weaknesses remaining. My overall impression is the impact of the manuscript will be limited by presentation style.

Response: Thank you for your kind comments. Based on your opinions and in conjunction with the concerns you mentioned in Question 1, we had refined this manuscript. The details are as follows:

First, we split this manuscript into two parts according to your requirements in the revised manuscript. Fig. 2-5 mainly described the results with "the preparation and functional characterization of RILO@MG", and Fig. 6-8 mainly describes the results with "the efficacy evaluation of preclinical animal models". According to your suggestion, we reduced some data in

the revised manuscript, which could ensure the integrity of this manuscript and highlight the key findings. The corresponding labels have been modified and improved. We hope these changes will meet your requirement.

Second, we added design rationale of valuating efficacy in the preclinical models in the revised manuscript. In order to investigate the antitumour effects of different preparations in an H22 tumour-bearing mouse model, thirteen groups were necessary and the main principles were as follows. NS group was set as the blank control group. For a start, we set up R848, INCB, RI, RLO, ILO and RILO groups to prove the advantages of combining TLR7/8 agonists with IDO1 inhibitor (compared R848 and INCB groups with RI group), nanomedicine delivery (compared R848 and INCB groups with RLO and ILO groups) and co-loading drugs into one nanoparticle (compared RI group with RILO group). Next, we set up Blank@M, LO@MG, RILO, combination treatment of RILO and MG (RILO+MG) and RILO@MG groups to prove the necessary for “inner packing” strategy. Lastly, RILO@M and RILO@MG- groups were used to demonstrate the role of “surface anchoring” strategy and releasing drugs in exosome form, respectively. The experimental results were further described and discussed to greatly improve reader appreciation of our findings in the revised manuscript.

Third, according to your suggestion, we simplified some results by focusing on necessary data on the basis of the antitumour evaluation in H22 tumour-bearing mouse model. The analysis of immune cells infiltration in Fig. 7 was set to the following eight groups (NS, Blank@M, LO@MG, RILO, RILO@M, RILO@MG-, RILO+MG and RILO@MG), and the experimental results were further described and discussed. We hope these changes will meet the requirement. The revised description had been supplemented in the manuscript and marked in red in the revised manuscript.

The revised parts were listed below:

The revised parts were consistent with that shown in Question 1.

REVIEWERS' COMMENTS

Reviewer #2 (Remarks to the Author):

Thank you for the additional revisions.

Reviewer #4 (Remarks to the Author):

In this second revision, the authors have improved the description and justification for their many treatment groups, reduced 39 supplemental figures to 20, and fixed some mistakes with statistics (normality of variance). The anti-tumor nanoparticle strategy remains of potentially high biomedical significance. However, the manuscript will be difficult to fully interpret. The overall amount of data was not reduced. Instead, the number of supplemental figures decreased because they were compressed into multi-panel figures. As a result, the target audience may overlook the key findings. Further, many experiments still either misuse or misreport the statistical method. How is One-Way ANOVA used to compare multiple curves in Figure 3b, as one example? Is each sample across the time series from an independent animal? It is more typical to see Two-Way repeated measures ANOVA for these types of studies.Further, the authors may not have understood concerns with use of statistics. Figures 3b-c, 6b, 7m, 8b, S5a, S5c, S6a-b, S10b, S17c, have time series data comparing multiple treatment groups using a One-Way ANOVA. It is unclear how the authors are comparing the curves with this multi-factor data. And it is unclear how the authors account for repeated measures on the same data. This was my meaning with "basic misunderstanding on ANOVA" and the "statistical assumptions or normal distribution or independent samples." Figure 5d also has comparisons across more than two treatments, but is analyzed with a One-Way ANOVA.

The Point-by-point Response to the Reviewers' Comments

Response to Reviewer#4 Comments:

In this second revision, the authors have improved the description and justification for their many treatment groups, reduced 39 supplemental figures to 20, and fixed some mistakes with statistics (normality of variance). The anti-tumor nanoparticle strategy remains of potentially high biomedical significance.

1. However, the manuscript will be difficult to fully interpret. The overall amount of data was not reduced. Instead, the number of supplemental figures decreased because they were compressed into multi-panel figures. As a result, the target audience may overlook the key findings.

Response: Thank you for your kind comments. According to your suggestion, we reduced some data in the revised manuscript (including Supplementary Fig. 3c, 5d, 5e, 9a, 9b, 17b, 17c, 18a and 18d in the previous manuscript), which could ensure the integrity of this manuscript and highlight the key findings. The corresponding labels have been modified and improved. We hope these changes will meet your requirement.

2. Further, many experiments still either misuse or misreport the statistical method.How is One-Way ANOVA used to compare multiple curves in Figure 3b, as one example? Is each sample across the time series from an independent animal?

It is more typical to see Two-Way repeated measures ANOVA for these types of studies. Further, the authors may not have understood concerns with use of statistics. Figures 3b-c, 6b, 7m, 8b, S5a, S5c, S6a-b, S10b, S17c, have time series data comparing multiple treatment groups using a One-Way ANOVA. It is unclear how the authors are comparing the curves with this multi-factor data. And it is unclear how the authors account for repeated measures on the same data. This was my meaning with "basic misunderstanding on ANOVA" and the "statistical assumptions or normal distribution or independent samples." Figure 5d also has comparisons across more than two treatments, but is analyzed with a One-Way ANOVA.

Response: Thank you for your kind comments. In the previous manuscript, we performed the one-way ANOVA using the data from the study endpoints, taking figure 3b as an example, we used the data from the 72nd hour instead of the entire curves for one-way ANOVA to demonstrate the cumulative release of

different formulations at 72 h. According to your suggestion, we revised the relevant statistical method. We revised the statistical significance using two-way ANOVA in the revised manuscript, including figures 3b-c, 5d, S5 and S6a-b. We revised the statistical significance using two-way ANOVA with repeated measures in the revised manuscript, including figures 6b, 7m, 8b, S10b and S17c (equivalent to figure 7m in the revised manuscript).

The figure 3b belongs to the in vitro experiment and 3 biologically independent experiments were repeated. We conducted the release profiles from different formulations according to the references published by Nature Portfolio (Nat Nanotechnol, 2023, 18, 647-656[1]; Nat Nanotechnol, 2021, 16, 104-113[2]). The specific steps were mentioned in the part of "Methods": in order to obtain the total drug release profiles from different formulations prepared using macrophages, R@MG, I@MG, RILO@MG- or RILO@MG was incubated with DMEM for 0.5, 1, 2, 4, 8, 12, 24, 48 or 72 h. The supernatant sample was collected, and fresh medium was added quickly at predetermined time points until 72 h. The amount of total R848 or INCB released into the supernatant was determined using HPLC.

For the in vivo experiments using animals. Taking figure 6b as an example, each curve across the time series contained data from 6 biologically independent animals. The specific steps were mentioned in the part of "Methods": the tumour length (L) and tumour width (W) were monitored every 2 days after the first treatment. In figure 6b, a total of 10 times were monitored over an 18-day time series for each independent animal.

Thank you very much for your reminder. We revised the statistical significance using two-way ANOVA, including figures 3b-c, 5d, S5 and S6a-b. We revised the statistical significance using two-way ANOVA with repeated measures, including figures 6b, 7m, 8b, S10b and S17c (equivalent to figure 7m in the revised manuscript). For two-way ANOVA with repeated measures, the main effect of group factor, the main effect of time factor, and the interaction between group and time had statistically significant on tumour volume ($P < 0.001$). The numerical data were matched between the figures and the source data. The revised description and figures had been supplemented in the manuscript and marked in red in the revised manuscript.

Reference:

[1] Luo Z, Lu Y, Shi Y, Jiang M, Shan X, Li X, Zhang J, Qin B, Liu X, Guo X, Huang J, Liu Y, Wang S, Li Q, Luo L, You J. Neutrophil hitchhiking for drug delivery to the bone marrow. Nat Nanotechnol. 2023,

18, 647-656.

[2] Shen S, Xu X, Lin S, Zhang Y, Liu H, Zhang C, Mo R. A nanotherapeutic strategy to overcome chemotherapeutic resistance of cancer stem-like cells. Nat Nanotechnol. 2021, 16, 104-113.

The revised parts were listed below:

24 Statistical analysis and schematic illustrations. GraphPad Prism 8 was used for statistical analyses. The data are expressed as the mean ± SD and the Shapiro-Wilk normality test was performed for evaluation of normal distribution. The data meet the homogeneity test of variance, the one-way ANOVA with Tukey's multiple comparisons test among multiple groups or two-tailed Student's t test among two groups was used for statistical significance calculation. The data do not meet the homogeneity test of variance, the Welch ANOVA with Dunnett's T3 multiple comparisons test among multiple groups or two-tailed Student's t test with Welch's correction among two groups was used for statistical significance calculation. The two-way ANOVA with Tukey's multiple comparisons test was used when two non-repeated measure parameters were considered. Further, the two-way ANOVA with repeated measures was used to analyze the effect of different formulations on tumour growth over time, the Geisser-Greenhouse correction was used when Mauchly's test of sphericity was not satisfied, and Tukey's post hoc test was used for inter-group comparison. $*P < 0.05$, $**P < 0.01$ and $***P < 0.001$ were considered statistically significant. Schematic illustrations of Fig. 1, 2a, 5a, 5i and 7a were created by ourselves with Adobe Illustrator. Schematic illustrations of Fig. 3a, 5g, 5k, 6a, 7k, 8a, 8i and Supplementary Fig. 3a were created by ourselves with Microsoft PowerPoint 2021 using icons from Biorender.com (Agreement number: CN25R9Z54P).

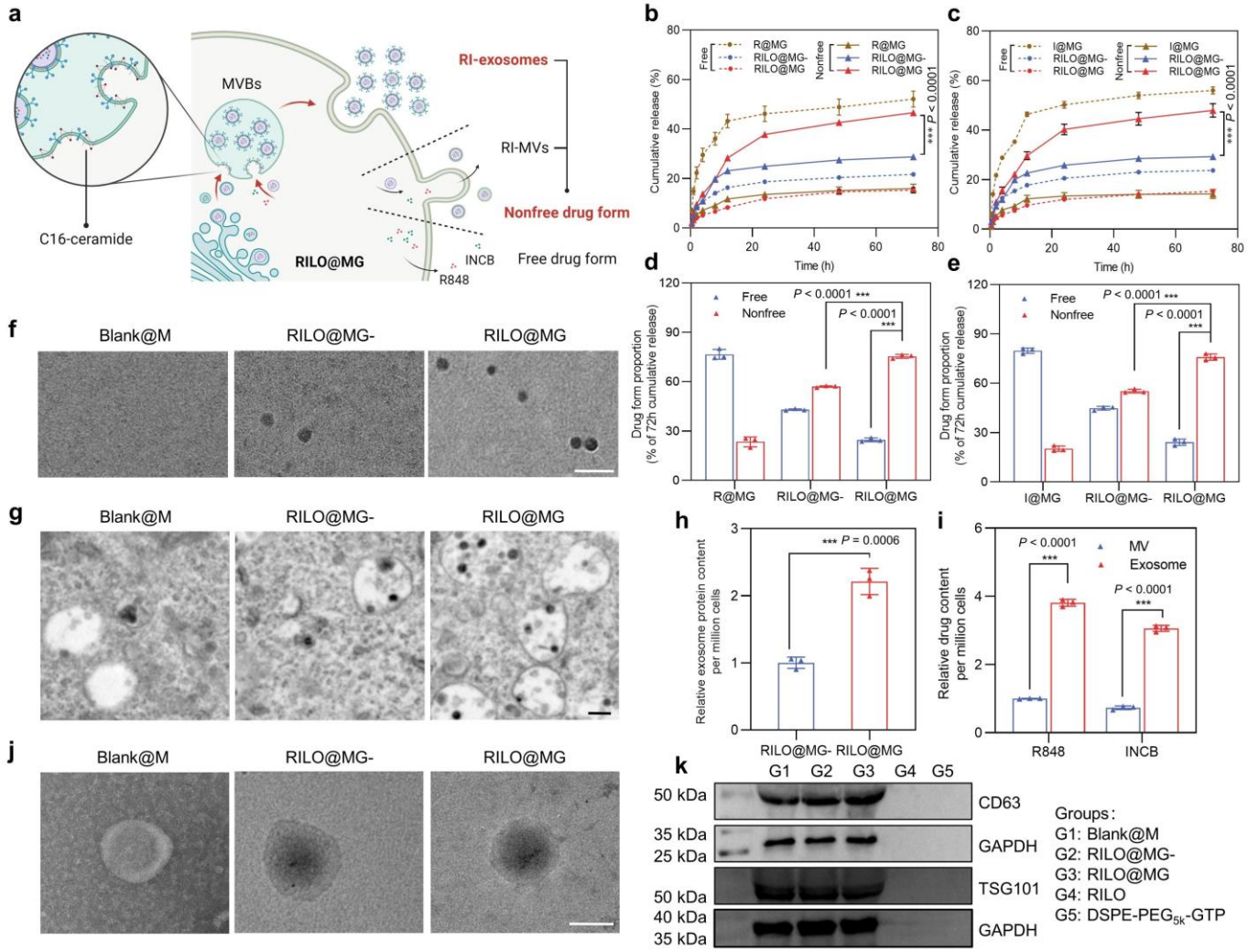

Fig. 3| RILOs are released from RILO@MG in the form of RI-exosomes. a, Schematic illustration of regulating the

release form of the RILOs packed in RILO@MG. **b-e,** Release profiles during 72 h for R848 (**b**) or INCB (**c**) and the proportion of cumulative release at 72 h for R848 (**d**) or INCB (**e**) of free drug form or nonfree drug form from different groups, respectively (n = 3 biologically independent experiments). **f,** Representative TEM analyses about released media from Blank@M, RILO@MG- and RILO@MG groups at 24 h after preparation (n = 3 biologically independent experiments). Scale bar, 200 nm. **g,** Representative TEM images showed increasing MVBs and ILVs formation containing RILO in RILO@MG with the help of C16-ceramide (n = 3 biologically independent experiments). Scale bar, 200 nm. **h,** The relative released exosome protein content 24 h after RILO@MG- and RILO@MG were prepared (n = 3 biologically independent experiments). **i,** R848 and INCB content encapsulated in exosomes or MVs by RILO@MG as measured by HPLC, indicating that the drugs were mostly contained in exosomes, not MVs (n = 3 biologically independent experiments). **j,** TEM images of exosomes from Blank@M and RI-exosomes from RILO@MG- and RILO@MG (n = 3 biologically independent experiments). Scale bar, 50 nm. **k,** Detection of exosome markers (CD63 and TSG101) of released exosomes from different groups by western blotting (n = 3 biologically independent experiments). Data are expressed as the mean ± SD. Two-tailed Student's t test (**d, e, h, i**) or two-way ANOVA with Tukey's multiple comparisons test (**b, c**) was carried out for statistical analysis. $^{*}P < 0.05$; $^{***}P < 0.001$. BMDMs were used in all experiments involving macrophages.

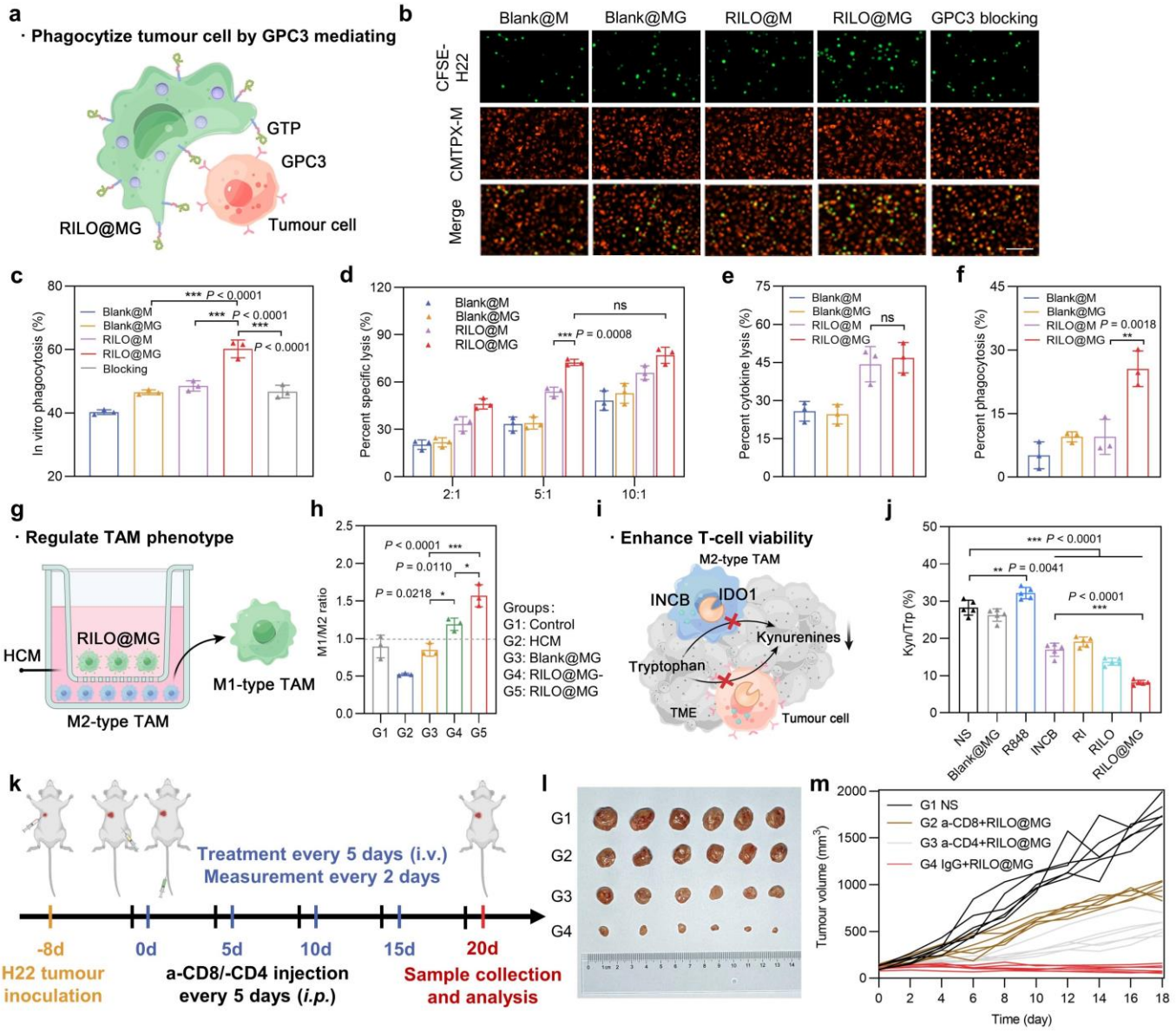

Fig. 5| RILO@MG promotes antitumour immunity by specifically phagocytizing tumour cells, regulating the TAM phenotype and enhancing T-cell viability. a, Schematic illustration of RILO@MG phagocytizing H22 cells mediated by GPC3 and GTP. **b,** Fluorescence microscopy images of different formulations after coculture with H22 cells for 4 hours (E:T = 2:1). Scale bar = 100 μm. E:T, effector cell (different formulations prepared using M1-type macrophage) to target cell (H22 cell) ratio. **c,** Anchoring of GTP on RILO@MG promoted the phagocytosis of H22 cells (n = 3 biologically independent experiments). Different formulations were cocultured with H22 cells for 4 h (E:T = 1:1) and evaluated by flow cytometric analysis. **d,** Specific lysis of H22 cells after coculture for 12 h at different E:T ratios measured by CCK-8 assay (n = 3 biologically independent experiments). **e, f,** Percent cytokine lysis (**e**) and phagocytosis lysis (**f**) of H22 cells after coculture with different formulations for 12 h (E:T = 5:1) by using Transwell plates (pore size 0.4 μm) (n = 3 biologically independent experiments). **g,** Experimental process for promoting the polarization from M2 phenotype to M1 phenotype. **h,** Phenotype analysis of TAMs after coculture with different formulations in HCM for 24 h (n = 3 biologically independent experiments). **i,** Schematic illustration of RILO@MG enhancing T cells by inhibiting the production of Kyn. **j,** IDO1 activity was evaluated according to the percentage of Kyn/Trp within tumours (n = 5 biologically independent animals per group). **k,** Regimen of the antitumour experiment after removal of $CD4^+$ or $CD8^+$ T cells. **l, m,** Photographs of tumours (**l**) and individual tumour growth curves (**m**) showed the critical role of T cells in antitumour immunity mediated by RILO@MG (n = 6 biologically independent animals per group). Data are expressed as

the mean ± SD and were processed by one-way ANOVA with Tukey's multiple comparisons test (**c, e-f, h, j**) or two-way ANOVA with Tukey's multiple comparisons test (**d**). **P* < 0.05; ***P* < 0.01; ****P* < 0.001; ns, no significance. BMDMs were used in all experiments involving macrophages.

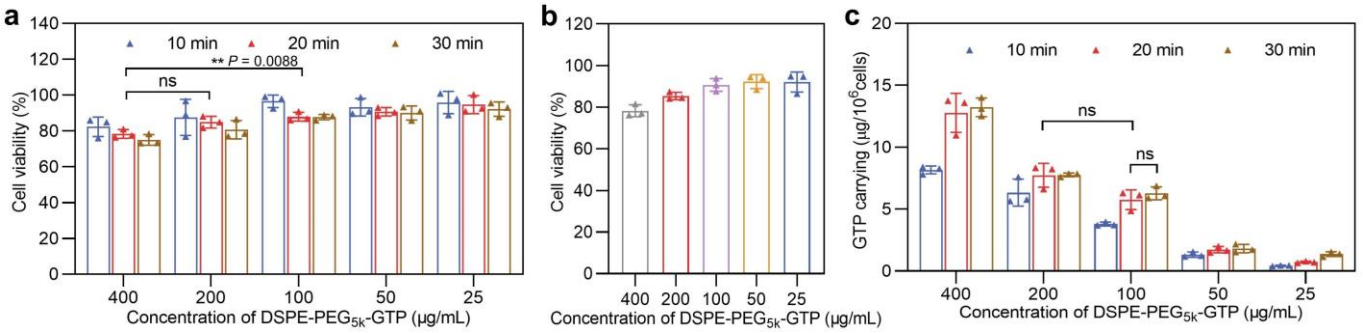

Supplementary Fig. 5. The optimizations of incubation concentrations and time on cell viability and GTP carrying. **a,** In vitro cell viability of different incubation concentrations and time of DSPE-PEG$_{5k}$-GTP on RILO@M^{RAW}. **b,** In vitro cell viability of different incubation concentrations of DSPE-PEG$_{5k}$-GTP on RILO@M^{BMDM} for incubating 20 min. **c,** The GTP carrying of different incubation concentrations and time of DSPE-PEG$_{5k}$-GTP on RILO@M^{RAW}. In addition, the GTP carrying of RILO@MG^{BMDM} was 6.67±0.64 μg/10^{6}cells at the optimal incubation concentration and time, which slightly higher than RILO@MG^{RAW} (5.76±0.79 μg/10^{6}cells). However, there was no significant difference between them, which were analysed by the two-tailed Student's *t*-test. Data are expressed as the mean ± SD with 3 biologically independent experiments. Two-way ANOVA with Tukey's multiple comparisons test (**a, c**) was carried out for statistical analysis. ***P* < 0.01; ns, no significance.

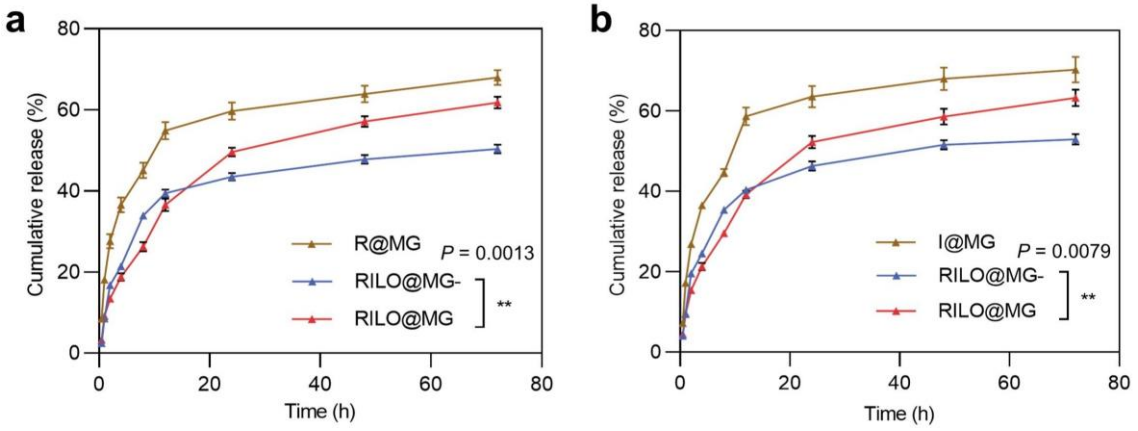

Supplementary Fig. 6. Release profiles of total drugs from RILO@MG. a, Release profiles during 72 h of total R848 from RILO@MG (*n* = 3 biologically independent experiments). **b,** Release profiles during 72 h of total INCB from RILO@MG (*n* = 3 biologically independent experiments). All data are shown as the mean ± SD and the data were analysed by two-way ANOVA with Tukey's multiple comparisons test. ***P* < 0.01.

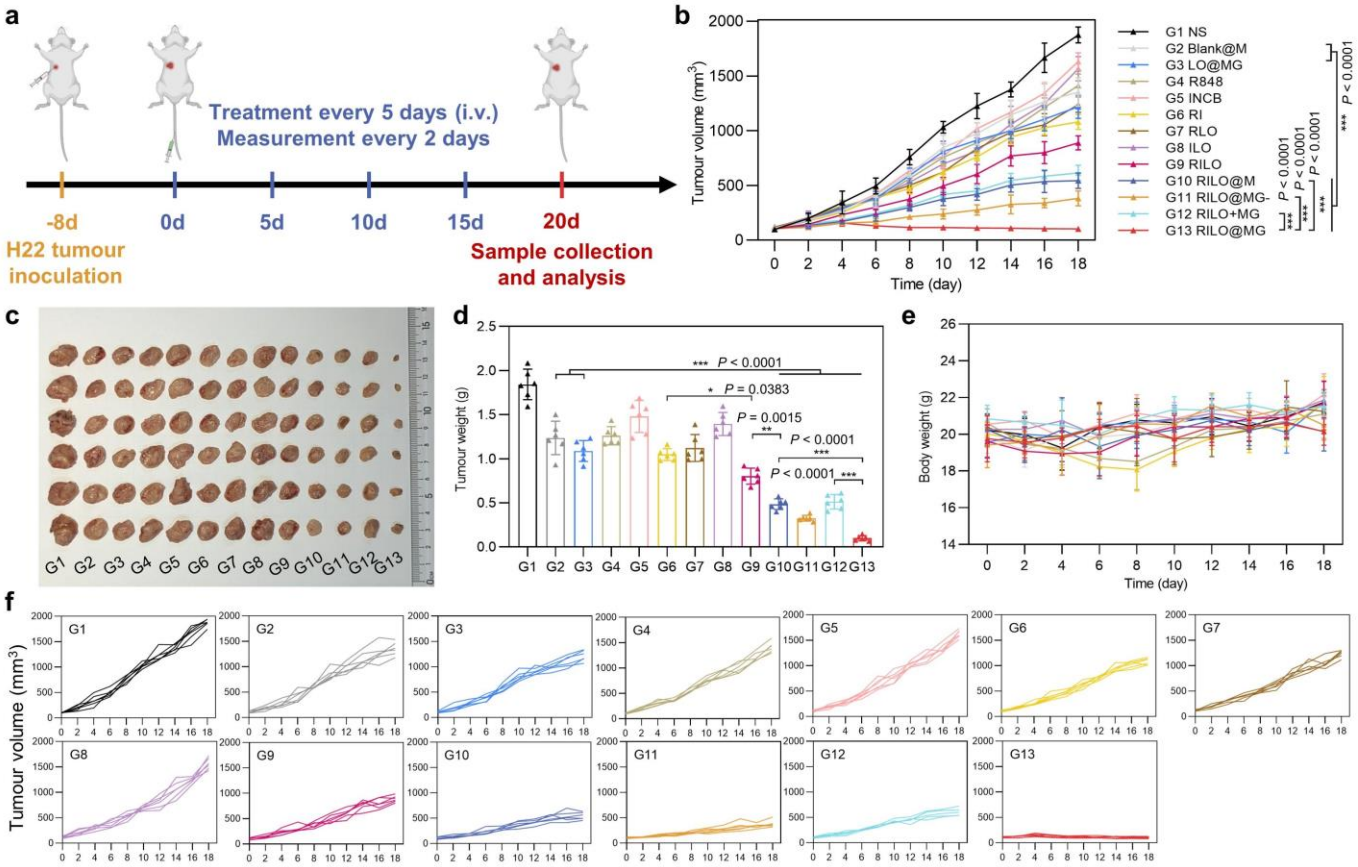

Fig. 6| The antitumour activity of RILO@MG in an H22 tumour-bearing mouse model. a, Regimen of i.v. administration in H22 tumour-bearing mice (at a dosage of 3.0×10^6 cells per mouse per injection, equal to 4 mg/kg R848 and 3.4 mg/kg INCB). Mice requiring injected formulations made by M1-type macrophages each received the equivalent number of cells (3.0×10^6 cells per mouse). Mice requiring injection of other formulations each received the equivalent dose of medicine (4 mg/kg R848 and 3.4 mg/kg INCB). When the tumour volumes reached ~2,000 mm^3, the mice were sacrificed. **b-f,** Average tumour growth curves (**b**), tumour photographs (**c**), tumour weights (**d**), body weight changes (**e**) and individual tumour growth curves (**f**) of H22 tumour-bearing mice receiving the indicated treatments (n = 6 biologically independent animals per group). Data are expressed as the mean ± SD. One-way ANOVA with Tukey's multiple comparisons test (**d**) or two-way ANOVA with repeated measures (**b**) was used for statistical analysis. *$P < 0.05$; **$P < 0.005$; ***$P < 0.001$. BMDMs were used in all experiments involving macrophages.

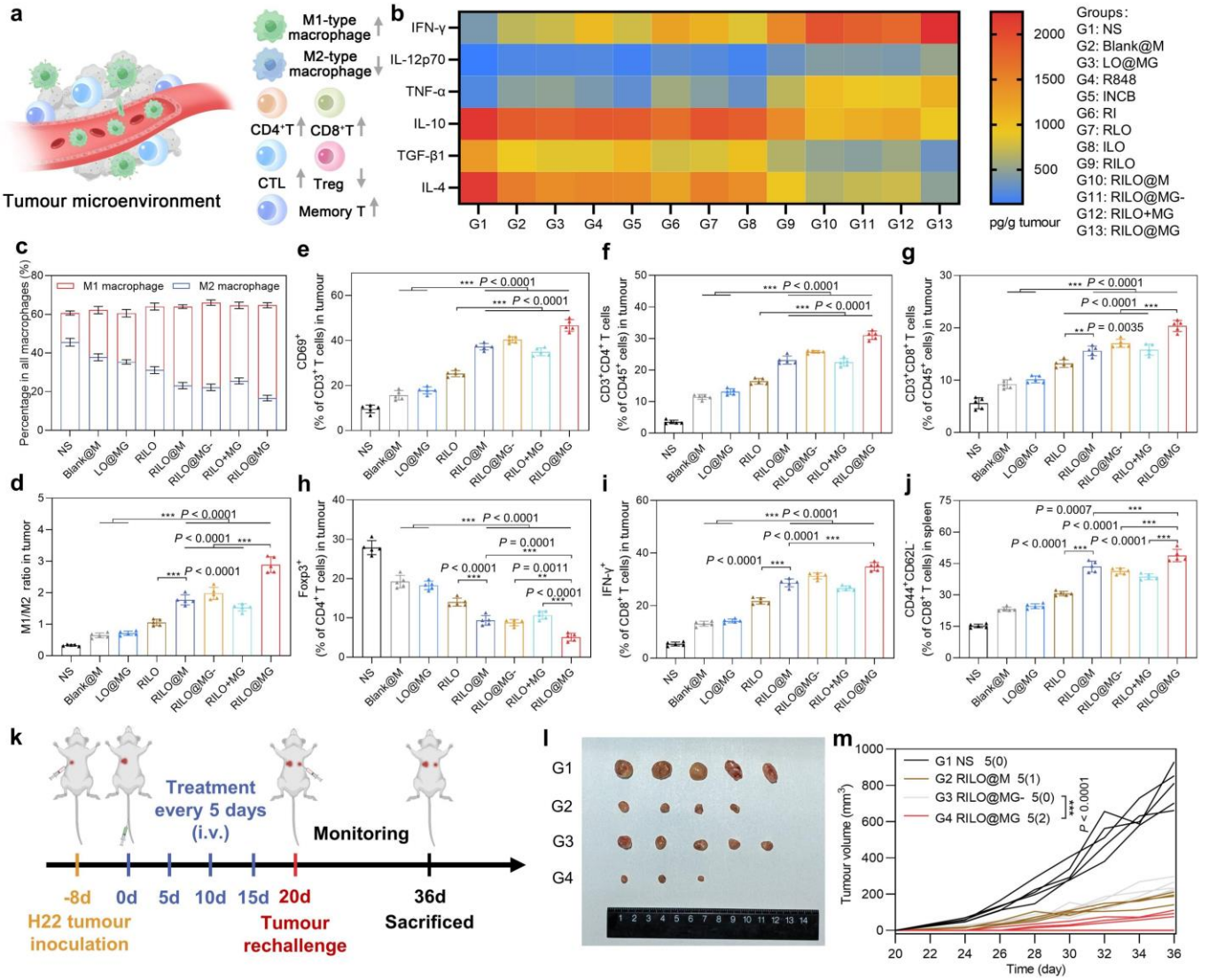

Fig. 7| The RILO@MG regulates TAM phenotype and enhances T-cell viability to remodel the suppressive TME in an H22 tumour-bearing mouse model. a, Schematic diagram of the regulatory effect of RILO@MG on the immunosuppressive TME, indicating an increase about immune-active cells and a decrease in the proportion of immune-suppressing cells within the TME. **b,** H22 tumour-bearing mice were treated as in Fig. 6a. The intratumoural levels of cytokines were quantified using ELISA analysis at the study endpoint. **c-i,** H22 tumour-bearing mice were treated as in Fig. 6a. Flow cytometric analysis of M1-type macrophage and M2-type macrophage (**c, d**), $CD69^+$ T cells (**e**), $CD4^+$ T cells (**f**), $CD8^+$ T cells (**g**), $CD4^+Foxp3^+$ T cells (**h**), and $CD8^+IFN\text{-}\gamma^+$ T cells (**i**) within the TME. **j,** Flow cytometric analysis quantification of effector memory ($CD44^+CD62L^-$) $CD8^+$ T cells in spleens. **k,** Experimental timeline of rechallenged tumour model establishment. **l,** Secondary tumour photographs of the sacrificed mice at the study endpoint. **m,** Rechallenged tumour growth curves of tumour-bearing mice were monitored over time. The dosage regimen of all data in Fig. 7 was the same as that shown in Fig. 6a. Data are expressed as the mean ± SD with 5 biologically independent animals per group and was processed by one-way ANOVA with Tukey's multiple comparisons test (**c-j**) or two-way ANOVA with repeated measures (**m**). $^{**}P < 0.01$; $^{***}P < 0.001$. BMDMs were used in all experiments involving macrophages.

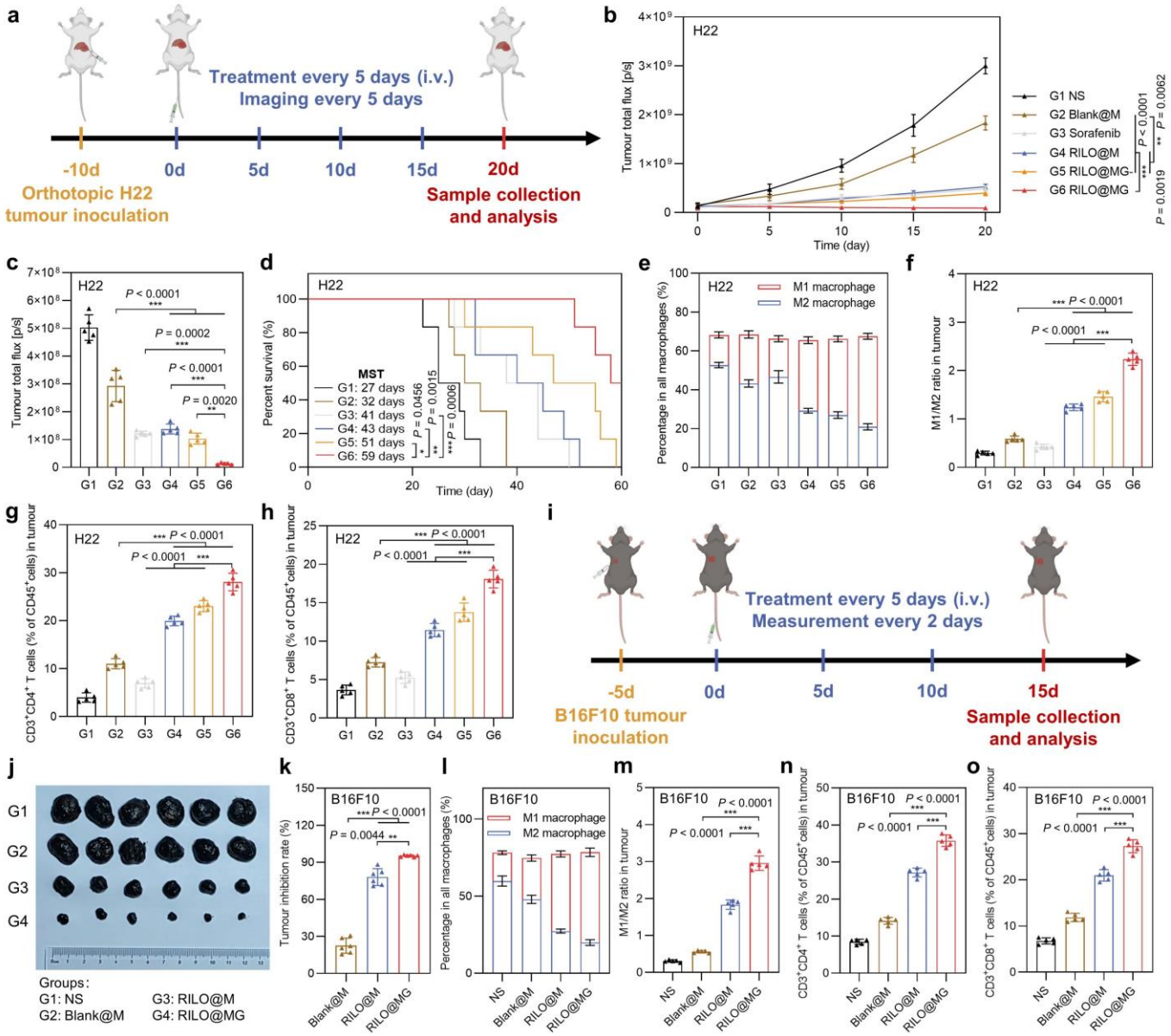

Fig. 8| Efficacy validation of RILO@MG in the orthotopic H22 tumour model and B16F10 tumour-bearing mouse model. a, Schematic of the orthotopic H22 tumour model experiment (dose of 3.0 × 10^6 cells per mouse per injection, equal to 4 mg/kg R848 and 3.4 mg/kg INCB; sorafenib: 10 mg/kg). **b-d,** In vivo bioluminescence intensity curves (**b**), ex vivo livers on Day 20 of bioluminescence quantification (**c**) and animal survival (**d**) of the orthotopic H22 tumour model receiving the indicated treatments (n = 5 biologically independent animals for **b-c** and n = 6 biologically independent animals for survival). **e-h,** Flow cytometry quantitative data of M1-type macrophage and M2-type macrophage (**e, f**) and $CD4^+$ and $CD8^+$ T cells (**g, h**) in tumours of the orthotopic H22 tumour model sacrificed on Day 20 (n = 5 biologically independent animals). **i,** Schematic of the B16F10 tumour-bearing mouse model experiment (dose of 3.0 × 10^6 cells per mouse per injection, equal to 4 mg/kg R848 and 3.4 mg/kg INCB). **j, k,** Tumour photographs (**j**) and tumour inhibition rate (**k**) of the sacrificed B16F10 tumour-bearing mice at the study endpoint (n = 6 biologically independent animals). **l-o,** Flow cytometry quantitative data of M1-type macrophage and M2-type macrophage (**l, m**) and $CD4^+$ and $CD8^+$ T cells (**n, o**) in tumours of the sacrificed B16F10 tumour-bearing mice (n = 5 biologically independent animals). Data are expressed as the mean ± SD. One-way ANOVA with Tukey's multiple comparisons test (**c, f-h, m-o**), the Welch ANOVA with Dunnett's T3 multiple comparisons test (**k**), two-way ANOVA with repeated measures (**b**) and log-rank tests for

survival data (**d**) were used for statistical analysis. $^{**}P < 0.01$; $^{***}P < 0.001$. BMDMs were used in all experiments involving macrophages.

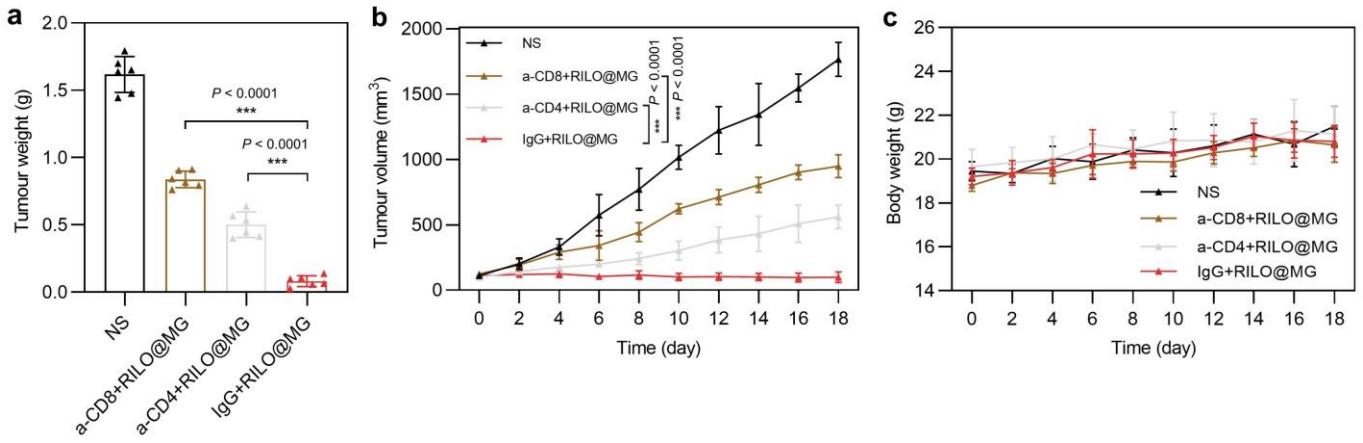

Supplementary Fig. 10. Tumour weights, average tumour growth curves and body weight changes over the course of treatment related to Fig. 5k-m. a, Tumour weights of H22 tumour-bearing mice (n = 6 biologically independent animals per group). **b**, Average tumour growth curves of H22 tumour-bearing mice (n = 6 biologically independent animals per group). **c,** body weight changes of H22 tumour-bearing mice (n = 6 biologically independent animals per group). All data are shown as the mean ± SD. One-way ANOVA with Tukey's multiple comparisons test (**a**) and two-way ANOVA with repeated measures (**b**) were carried out for statistical analysis. $^{***}P < 0.001$.